

Supporting Information

The First Examples of Cofacial Bis(dipyrins)

Jude Deschamps, Yi Chang, Adam Langlois, Nicolas Desbois, Claude P. Gros, Pierre D. Harvey

| | | |
|--------------------|--|-----|
| Figure S1. | ^1H NMR of BOD-OMe (3) (CDCl_3 , 298K) | S3 |
| Figure S2. | ^{13}C NMR of BOD-OMe (3) (CDCl_3 , 298K) | S3 |
| Figure S3. | ^1H NMR of BOD-O (4) (CDCl_3 , 298K). | S4 |
| Figure S4. | ^{13}C NMR of BOD-O (4) (CDCl_3 , 298K). | S4 |
| Figure S5. | ^1H NMR of 5a (CDCl_3 , 298K). | S5 |
| Figure S6. | ^{13}C NMR of 5a (CDCl_3 , 298K). | S5 |
| Figure S7. | ^1H NMR of 6a (CDCl_3 , 298K) | S6 |
| Figure S8. | ^{13}C NMR of 6a (CDCl_3 , 298K). | S6 |
| Figure S9. | ^1H NMR of DPO-OMe (7) (CDCl_3 , 298K). | S7 |
| Figure S10. | ^{13}C NMR of DPO-OMe (7) (CDCl_3 , 298K). | S7 |
| Figure S11. | ^1H NMR of DPA-OMe (8) (CDCl_3 , 298K). | S8 |
| Figure S12. | ^{13}C NMR of DPA-OMe (8) (CDCl_3 , 298K). | S8 |
| Figure S13. | ^1H NMR of DPO-O (9) (d_6 -acetone, 298K). | S9 |
| Figure S14. | ^{13}C NMR of DPO-O (9) (CDCl_3 , 298K). | S9 |
| Figure S15. | ^1H NMR of DPA-O (10) (d_6 -acetone, 298K). | S10 |
| Figure S16. | ^{13}C NMR of DPA-O (10) (d_6 -acetone, 298K). | S10 |
| Figure S17. | MALDI-TOF mass spectra of 1 . | S11 |
| Figure S18. | HRMS (ESI) mass spectra of BOD-OMe (3) . | S12 |
| Figure S19. | MALDI-TOF mass spectra of BOD-O (4) . | S13 |
| Figure S20. | HRMS (MALDI-TOF) mass spectra of 5a . | S14 |
| Figure S21. | MALDI-TOF mass spectra of 6a . | S15 |
| Figure S22. | HRMS (ESI) mass spectra of DPO-OMe (7) . | S16 |
| Figure S23. | HRMS (ESI) mass spectra of DPA-OMe (8) . | S17 |
| Figure S24. | HRMS (MALDI-TOF) mass spectra of DPO-O (9) . | S18 |
| Figure S25. | HRMS (MALDI-TOF) mass spectra of DPA-O (10) . | S19 |
| Procedure | DFT and TD-DFT calculation procedure | S20 |
| Figure S26. | Optimized geometries (DFT, B3LYP) for BOD-OMe (3) , BOD-O (4) , DPO-OMe (7) and DPO-O (9) . | S21 |
| Figure S27. | Optimized geometries (DFT, B3LYP) for DPO-O (9) , DPO-OMe (7) , DPA-O (10) and DPA-OMe (8) showing select structural parameters. | S22 |
| Figure S28. | Representations of the frontier MOs for BOD-O (4) . | S23 |
| Figure S29. | Representations of the frontier MOs for DPA-OMe (8) . | S23 |
| Figure S30. | Representations of the frontier MOs for DPO-O (9) . | S24 |
| Figure S31. | Representations of the frontier MOs for DPA-O (10) . | S24 |
| Table 1. | Percent distribution of the molecular orbitals over selected molecular fragments of DPA-OMe (8) | S25 |
| Table 2. | Percent distribution of the molecular orbitals over selected molecular fragments of DPO-O (9) | S25 |

| | | |
|--------------------|--|-----|
| Table 3. | Percent distribution of the molecular orbitals over selected molecular fragments of DPA-O (10) | S25 |
| Figure S32. | Electronic density map (DFT) for DPA-OMe (8) and DPA-O (10) . | S25 |
| Figure S33. | Graphs reported the computed oscillator strength (F) as a function of the calculated positions of the first 75 electronic transitions for BOD-O (4) (top), DPA-O (10) (middle) and DPO-O (9) (bottom) | S26 |
| Table 4. | Computed oscillator strengths (F), positions of the first electronic transitions and major contributions of BOD-OMe (3) | S27 |
| Table 5. | Computed oscillator strengths (F), positions of the first electronic transitions and major contributions of BOD-O (4) | S29 |
| Table 6. | Computed oscillator strengths (F), positions of the first electronic transitions and major contributions of DPO-OMe (7) | S31 |
| Table 7. | Computed oscillator strengths (F), positions of the first electronic transitions and major contributions of DPA-OMe (8) | S33 |
| Table 8. | Computed oscillator strengths (F), positions of the first electronic transitions and major contributions of DPO-O (9) | S35 |
| Table 9. | Computed oscillator strengths (F), positions of the first electronic transitions and major contributions of DPA-O (10) | S37 |
| Figure S34. | Fluorescence decay trace for BOD-OMe (3) at 298 and 77 K | S39 |
| Figure S35. | Fluorescence decay trace for BOD-O (4) at 298 and 77 K | S39 |
| Figure S36. | Fluorescence decay trace for DPO-OMe (7) at 298 and 77 K | S40 |
| Figure S37. | Fluorescence decay trace for DPA-OMe (8) at 298 and 77 K | S40 |
| Figure S38. | Fluorescence decay trace for DPO-O (9) at 298 and 77 K | S41 |
| Figure S39. | Fluorescence decay trace for DPA-O (10) at 298 and 77 K | S41 |
| Figure S40. | Evolution of fluorescence spectra of BOD-O (4) upon addition of C ₆₀ . | S42 |
| Figure S41. | Evolution of fluorescence spectra of DPO-OMe (7) upon addition of C ₆₀ . | S42 |
| Figure S42. | Evolution of fluorescence spectra of DPA-OMe (8) upon addition of C ₆₀ . | S42 |
| Figure S43. | Evolution of fluorescence spectra of DPO-O (9) upon addition of C ₆₀ . | S43 |
| Figure S44. | Evolution of fluorescence spectra of DPA-O (10) upon addition of C ₆₀ . | S43 |

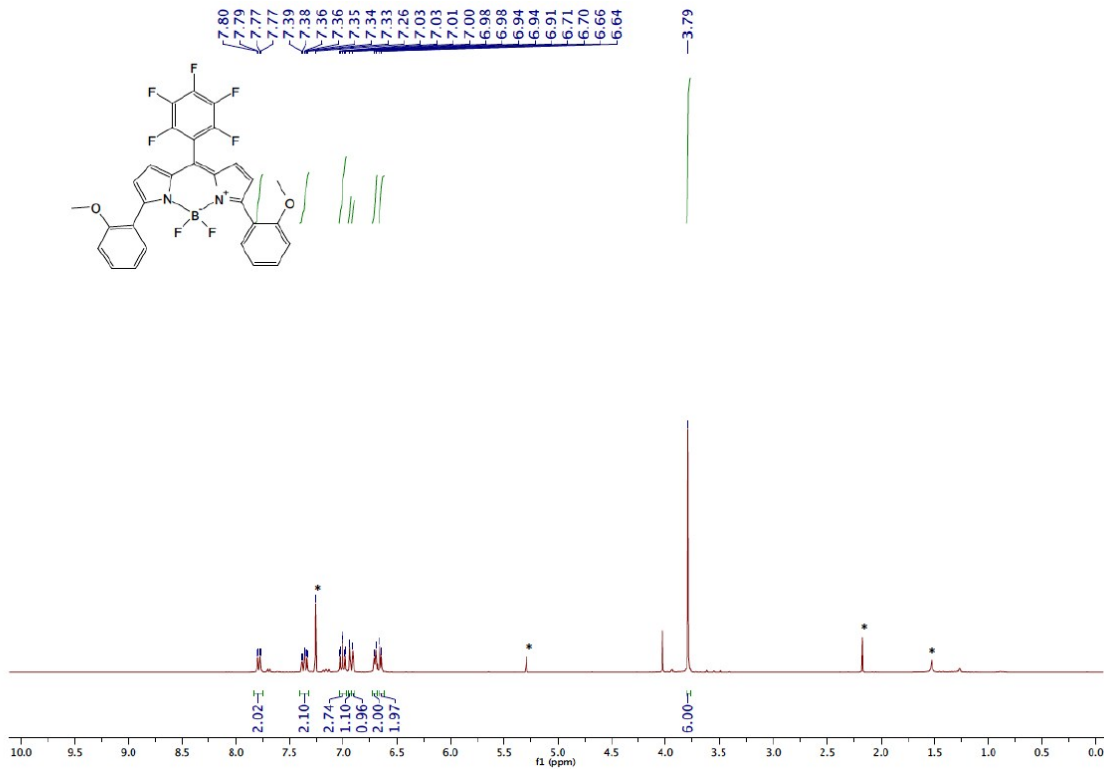


Figure S1. ^1H NMR of BOD-OMe (3) (CDCl_3 , 298K).

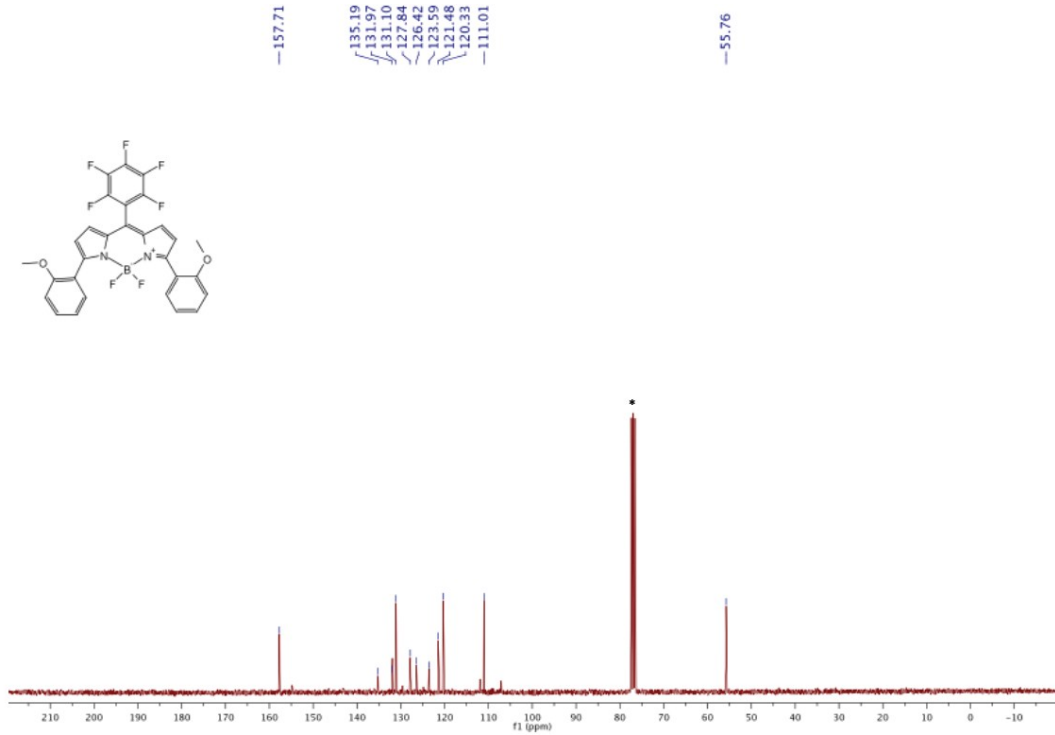


Figure S2. ^{13}C NMR of BOD-OMe (3) (CDCl_3 , 298K).

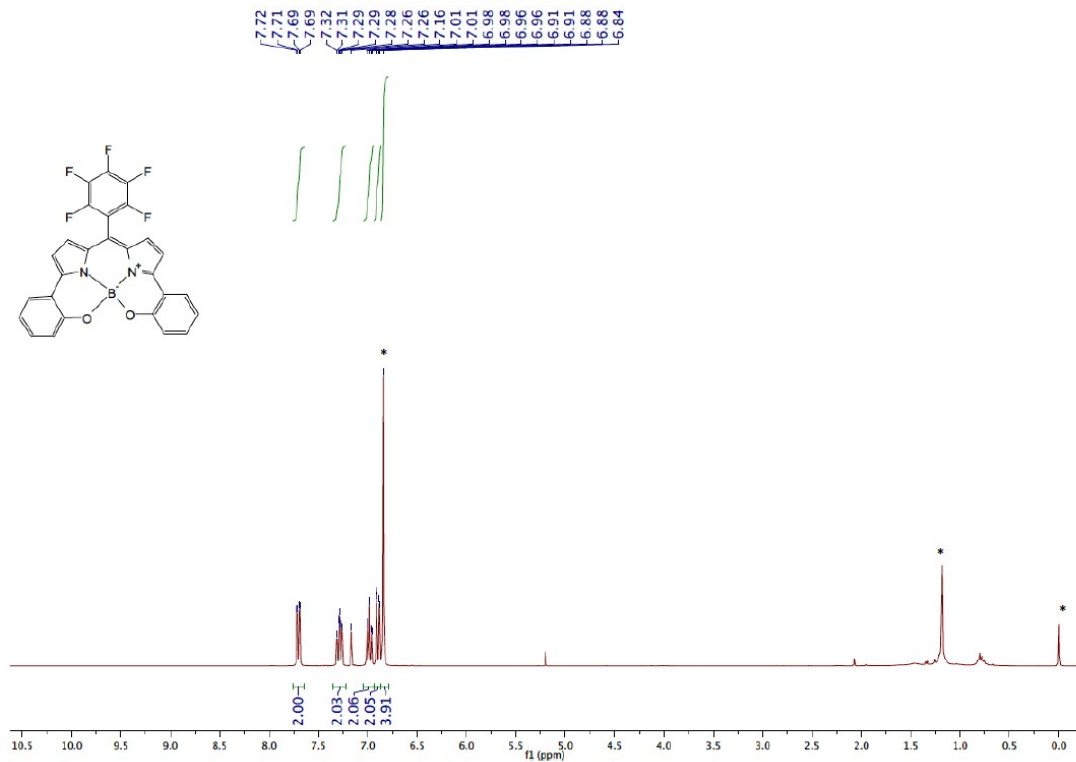


Figure S3. ^1H NMR of **BOD-O (4)** (CDCl_3 , 298K).

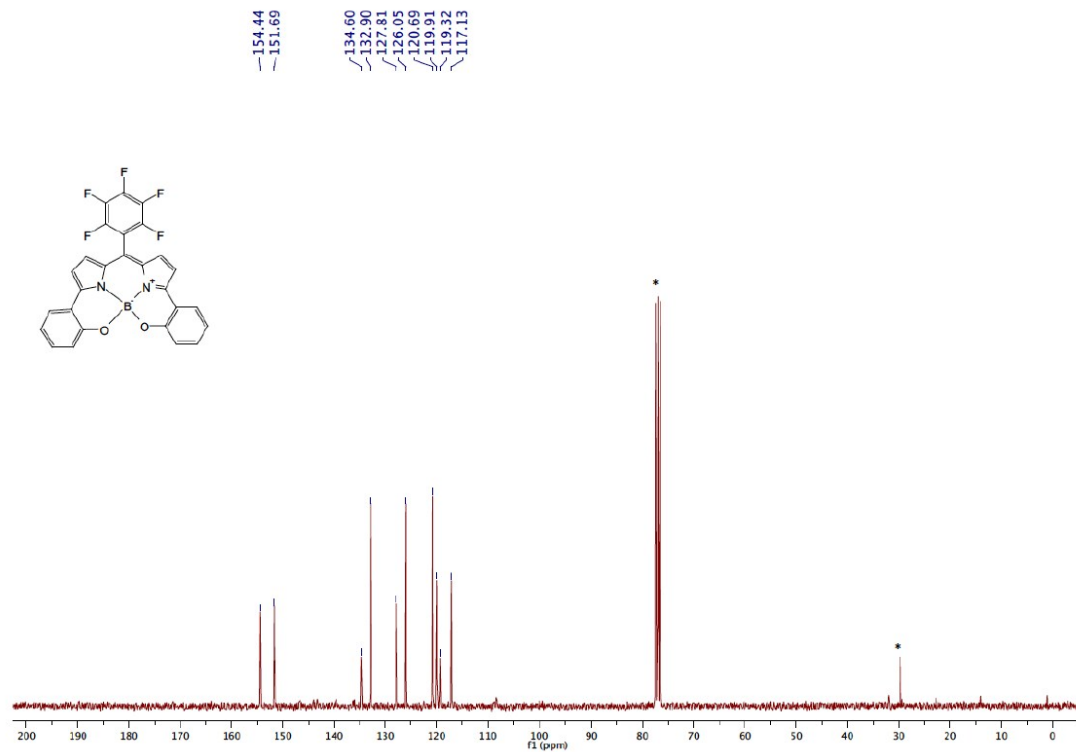


Figure S4. ^{13}C NMR of **BOD-O (4)** (CDCl_3 , 298K).

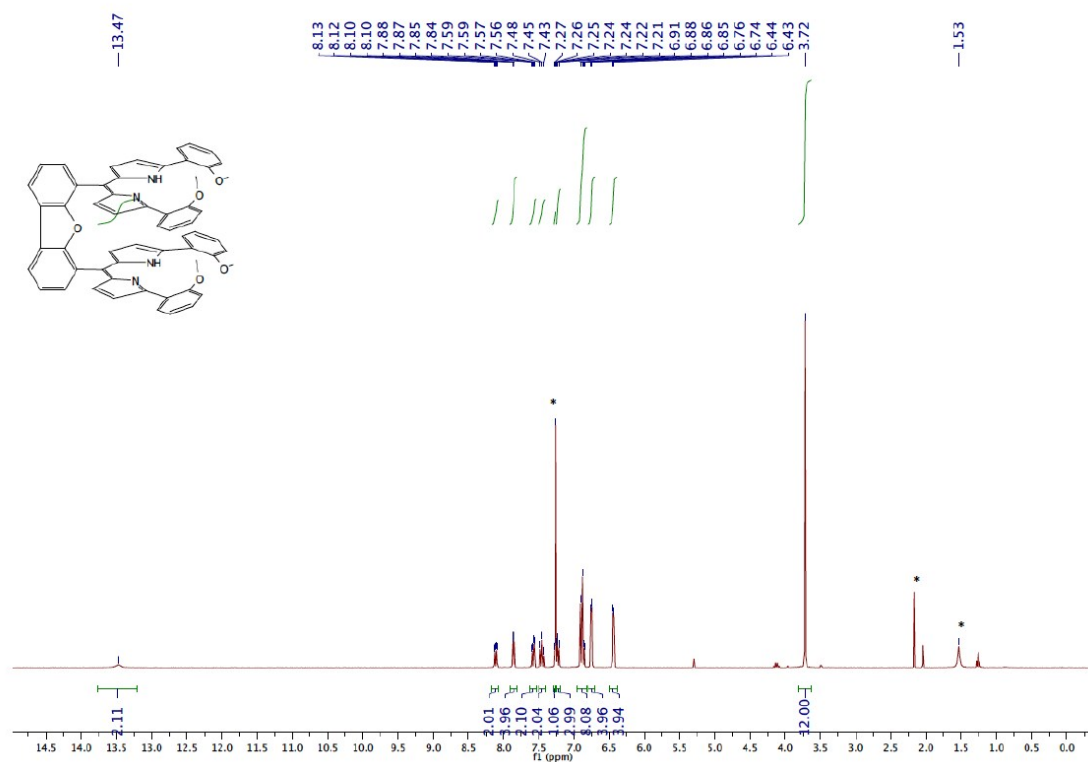


Figure S5. ^1H NMR of **5a** (CDCl_3 , 298K).

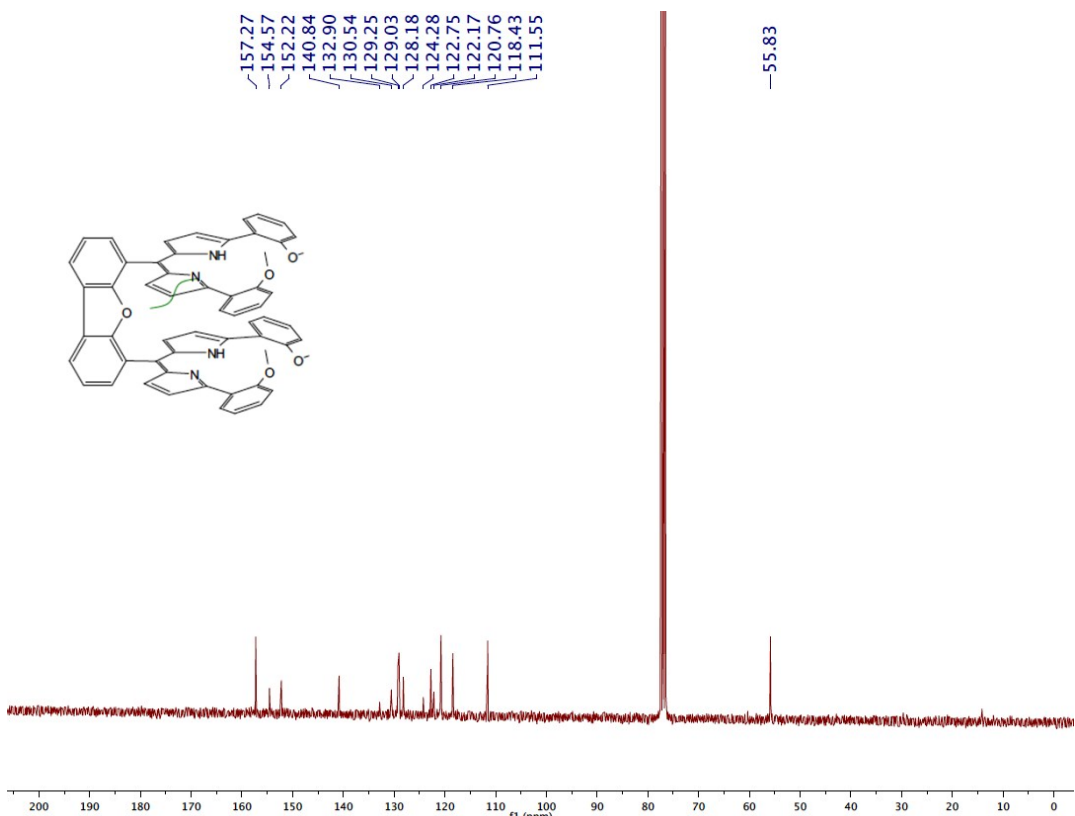


Figure S6. ^{13}C NMR of **5a** (CDCl_3 , 298K).

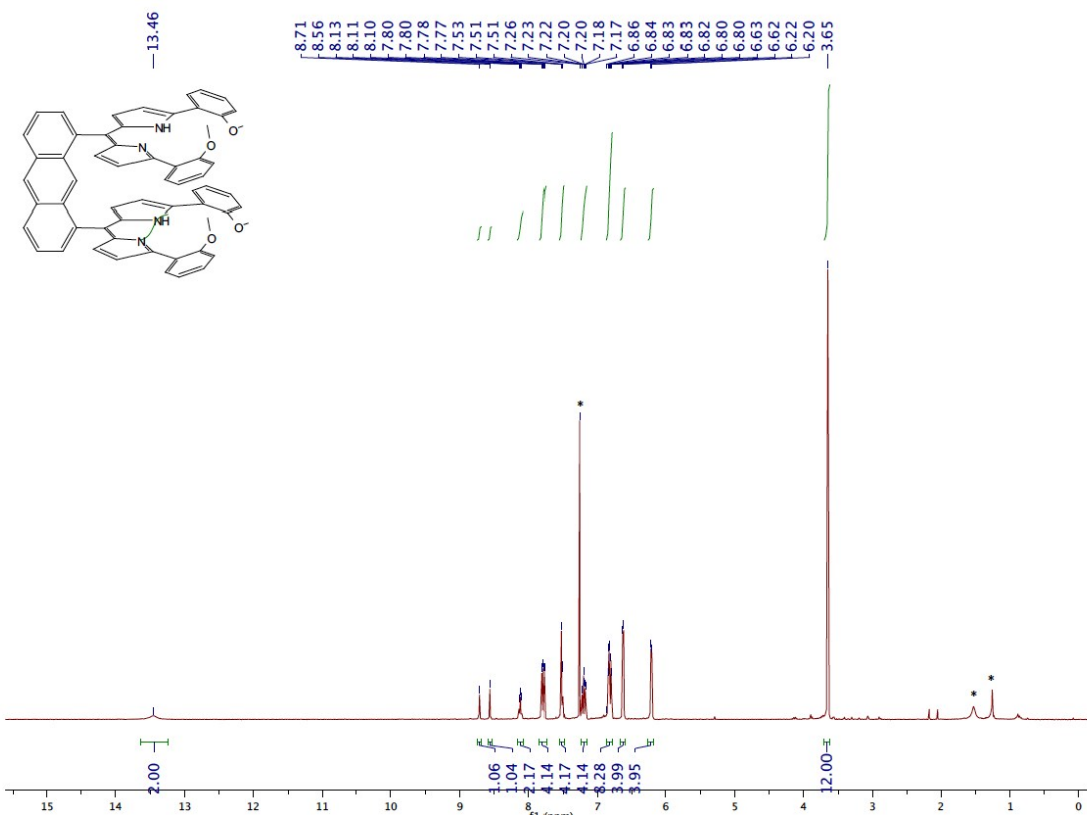


Figure S7. ^1H NMR of **6a** (CDCl_3 , 298K).

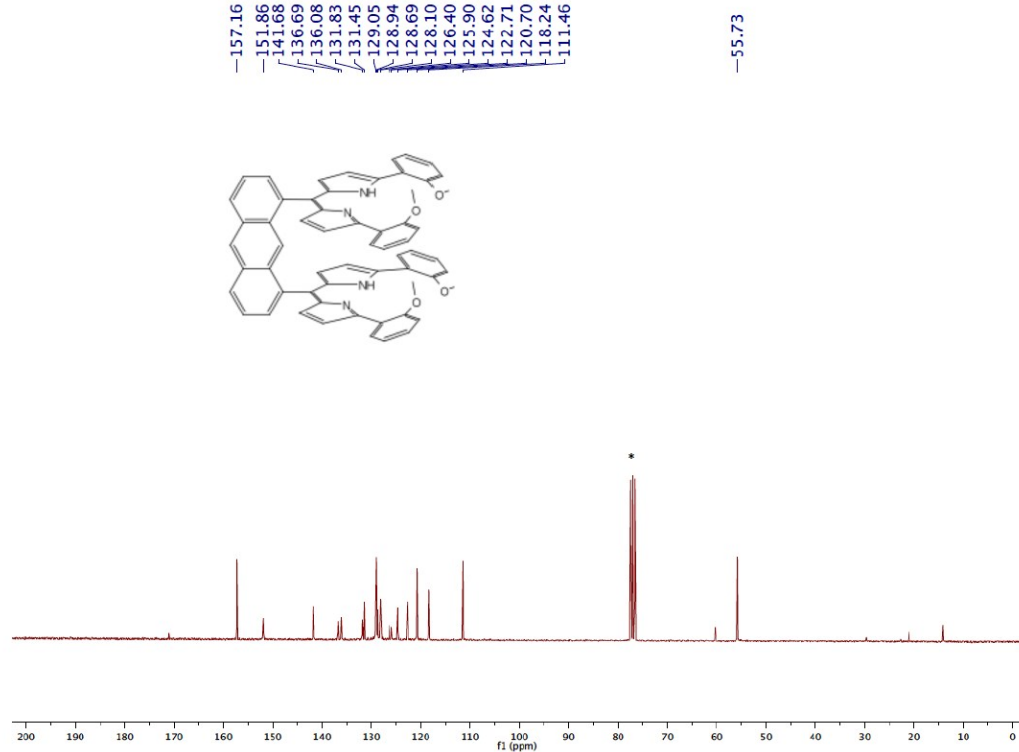


Figure S8. ^{13}C NMR of **6a** (CDCl_3 , 298K).

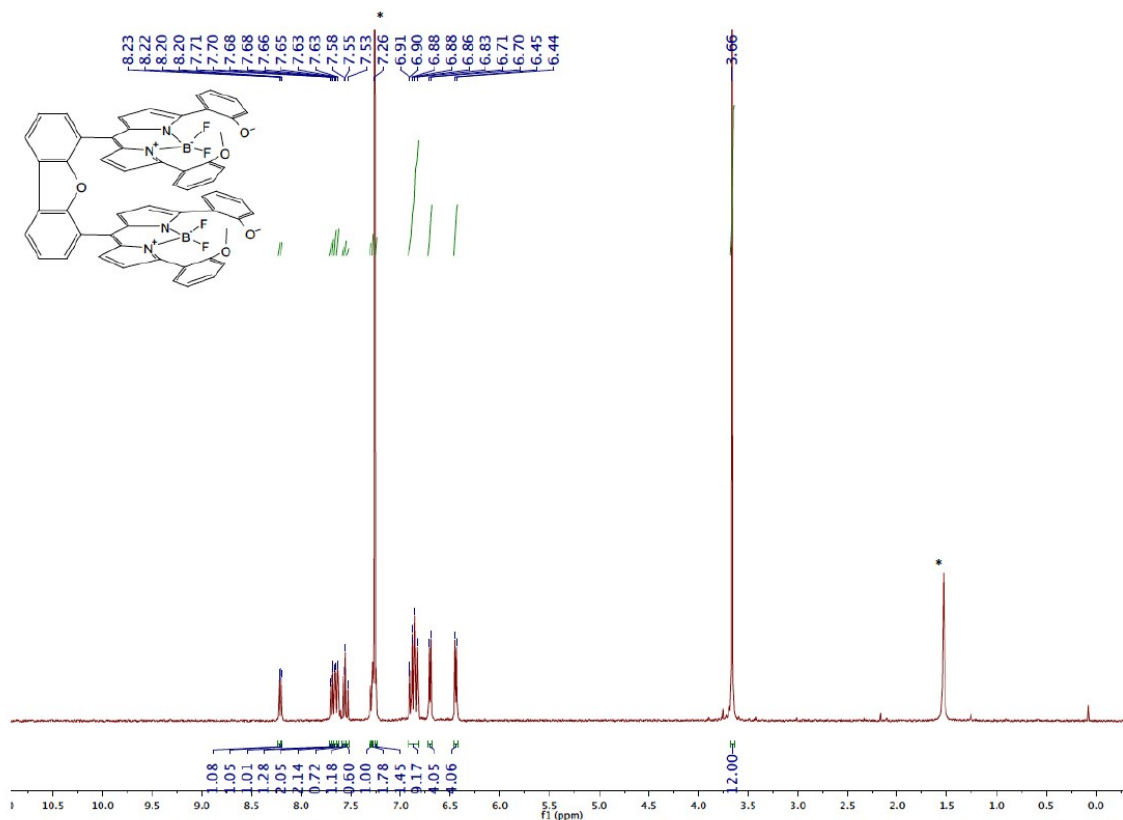


Figure S9. ^1H NMR of **DPO-OMe (7)** (CDCl_3 , 298K).

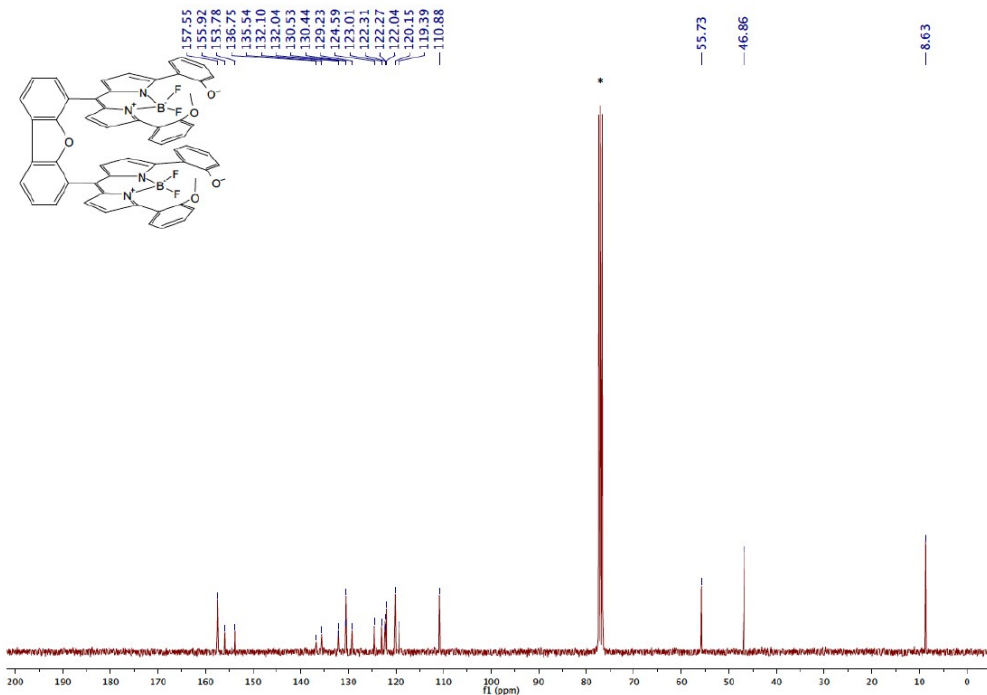


Figure S10. ^{13}C NMR of DPO-OMe (7) (CDCl_3 , 298K).

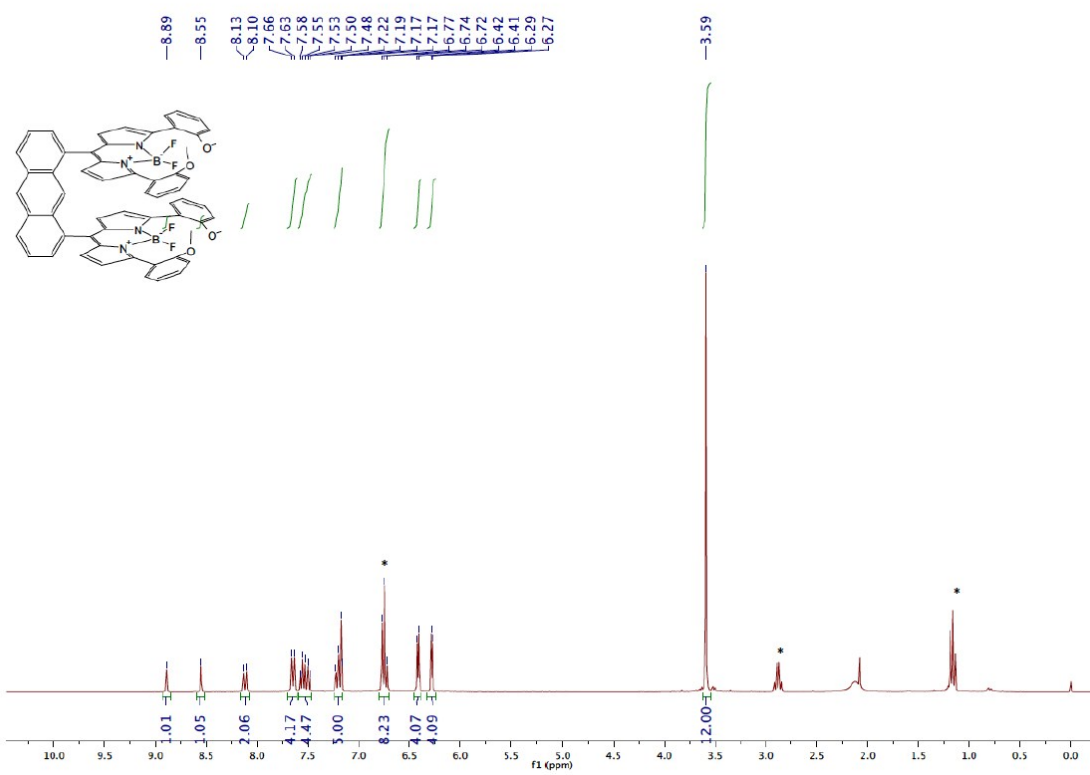


Figure S11. ¹H NMR of **DPA-OMe (8)** (CDCl_3 , 298K).

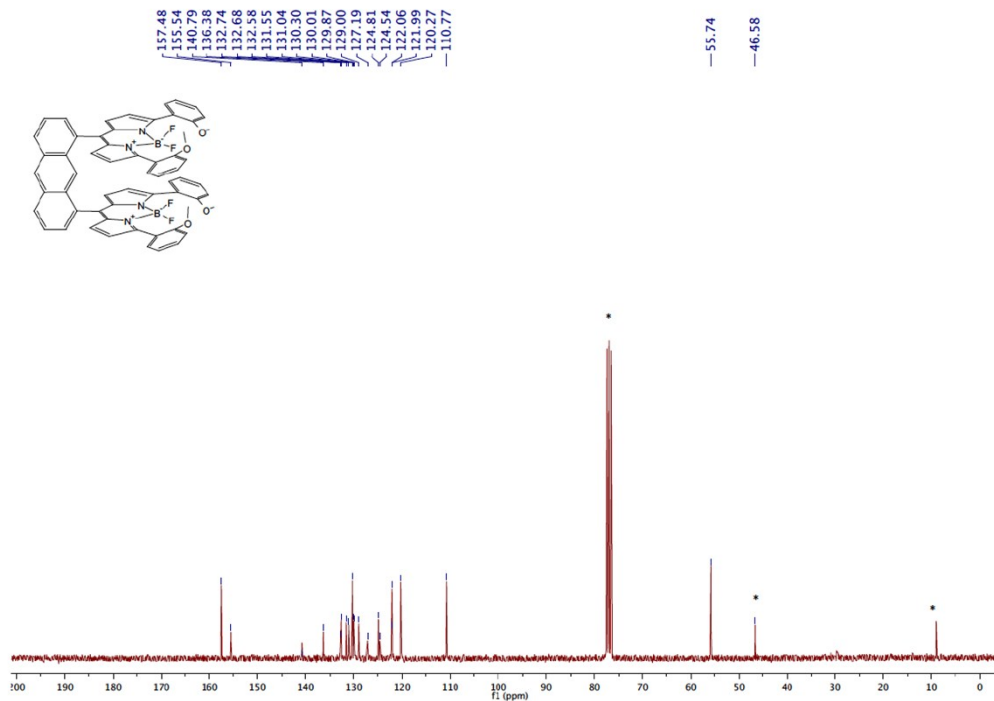


Figure S12. ¹³C NMR of **DPA-OMe (8)** (CDCl_3 , 298K).

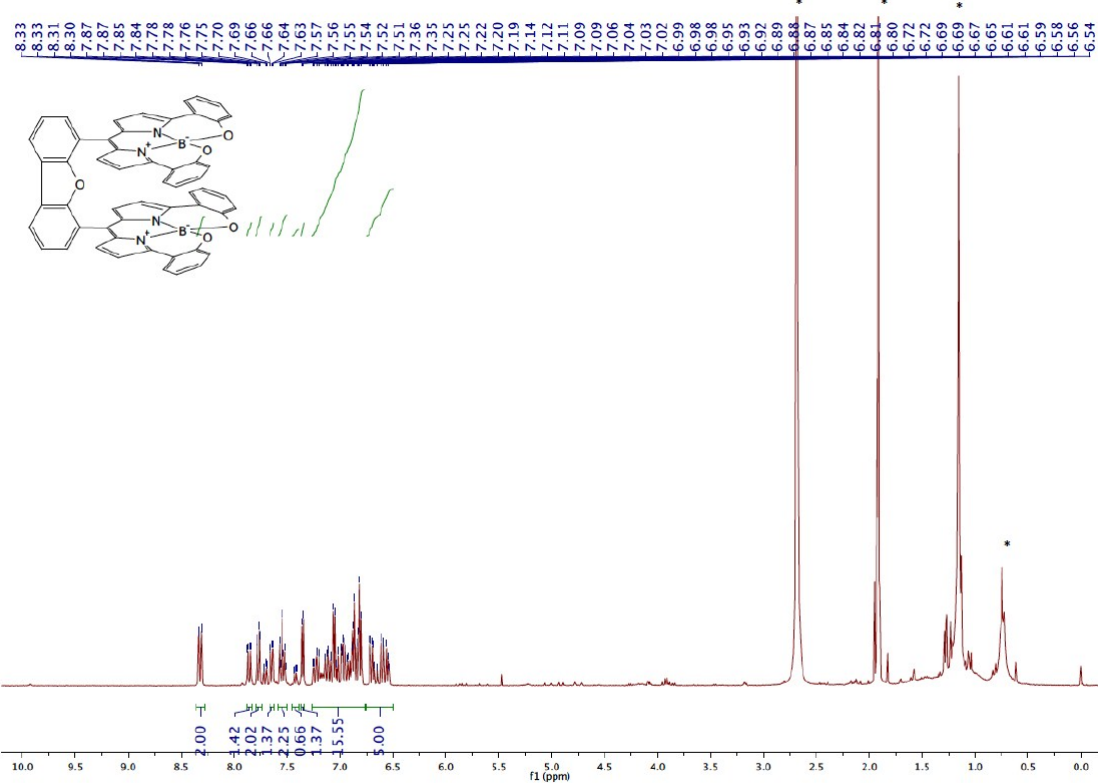


Figure S13. ¹H NMR of DPO-O (9) (d_6 -acetone, 298K).

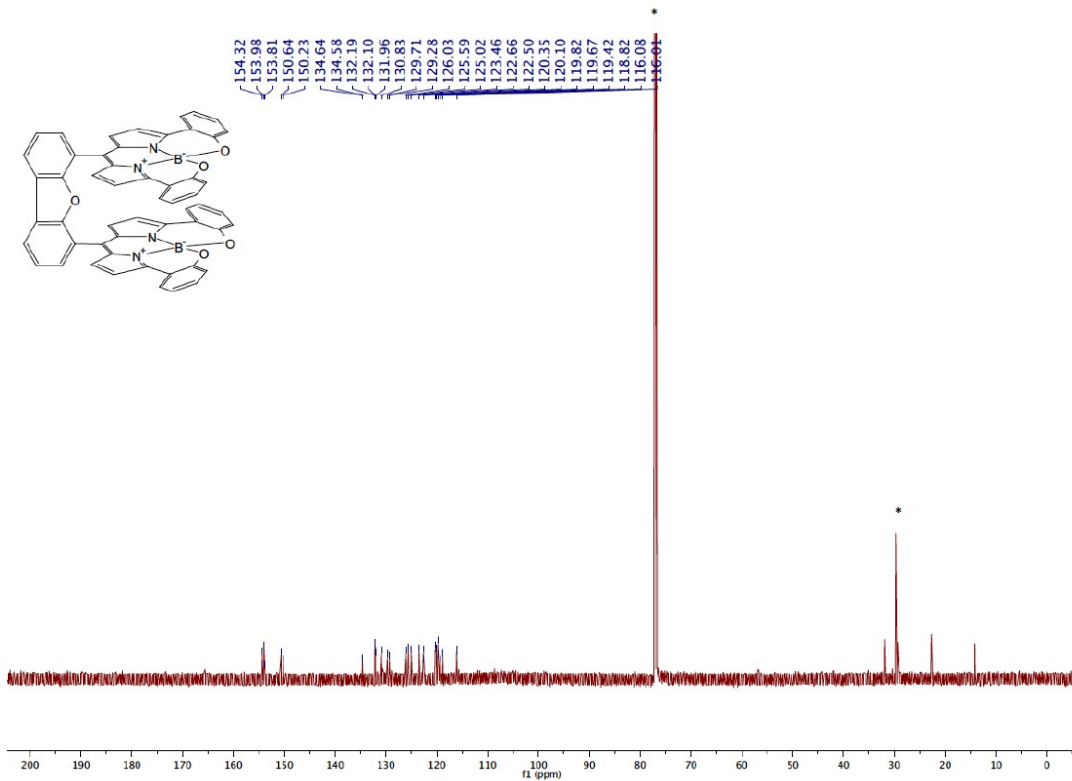


Figure S14. ¹³C NMR of DPO-O (9) ($CDCl_3$, 298K).

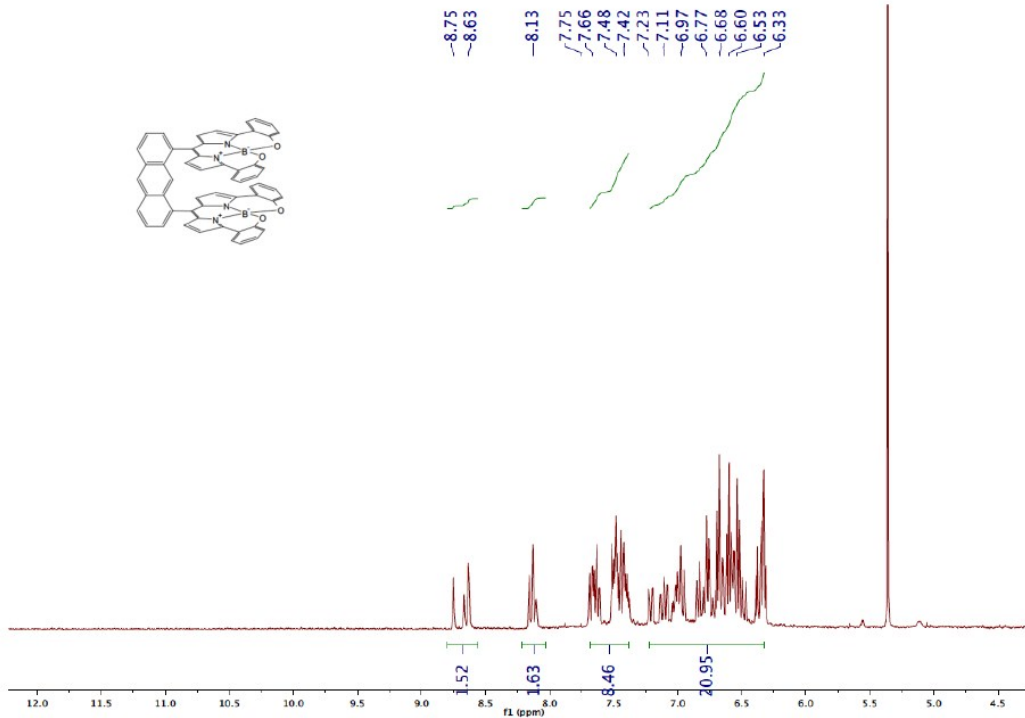


Figure S15. ^1H NMR of **DPA-O (10)** (d_6 -acetone, 298K).

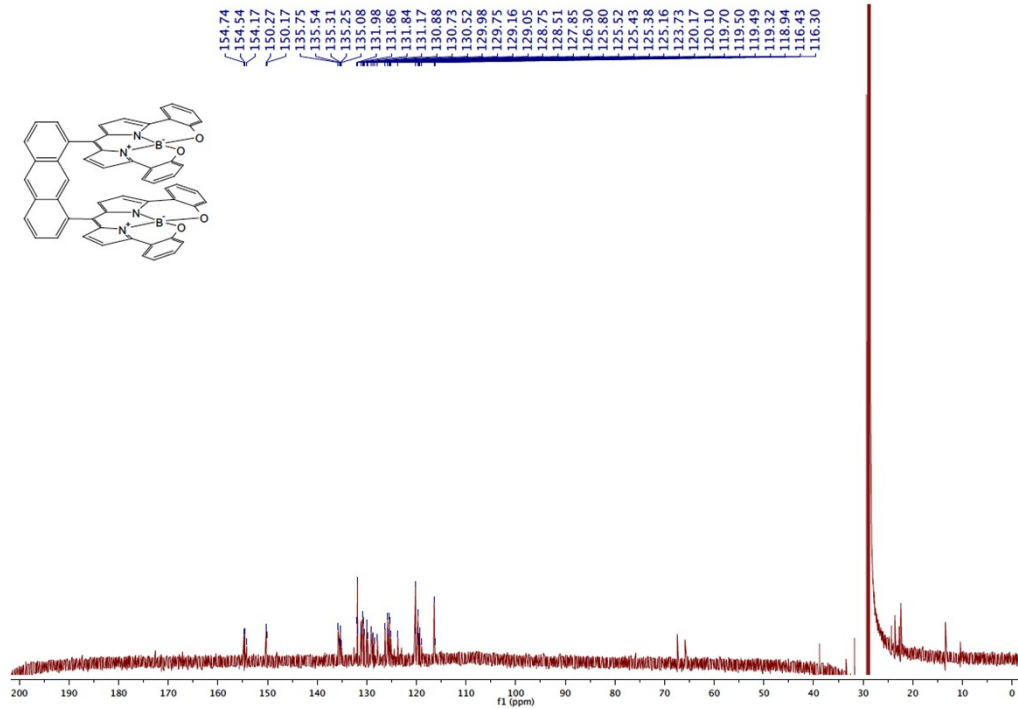
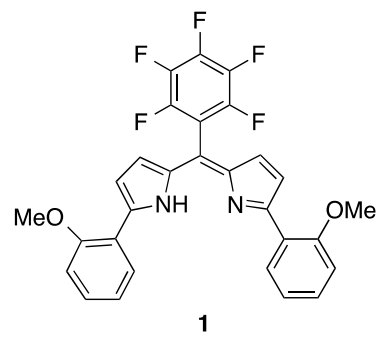
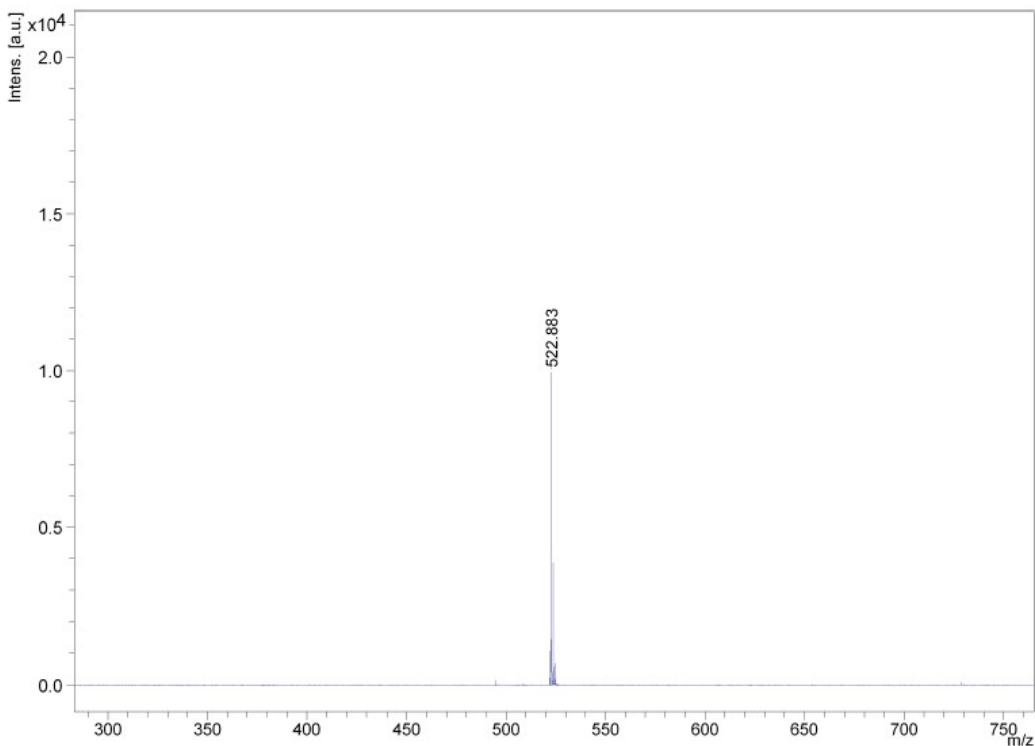


Figure S16. ^{13}C NMR of **DPA-O (10)** (d_6 -acetone, 298K).



Chemical Formula: C₂₉H₁₉F₅N₂O₂
Exact Mass: 522.1367
Molecular Weight: 522.4750

Figure S17. MALDI-TOF mass spectrum of **1**.

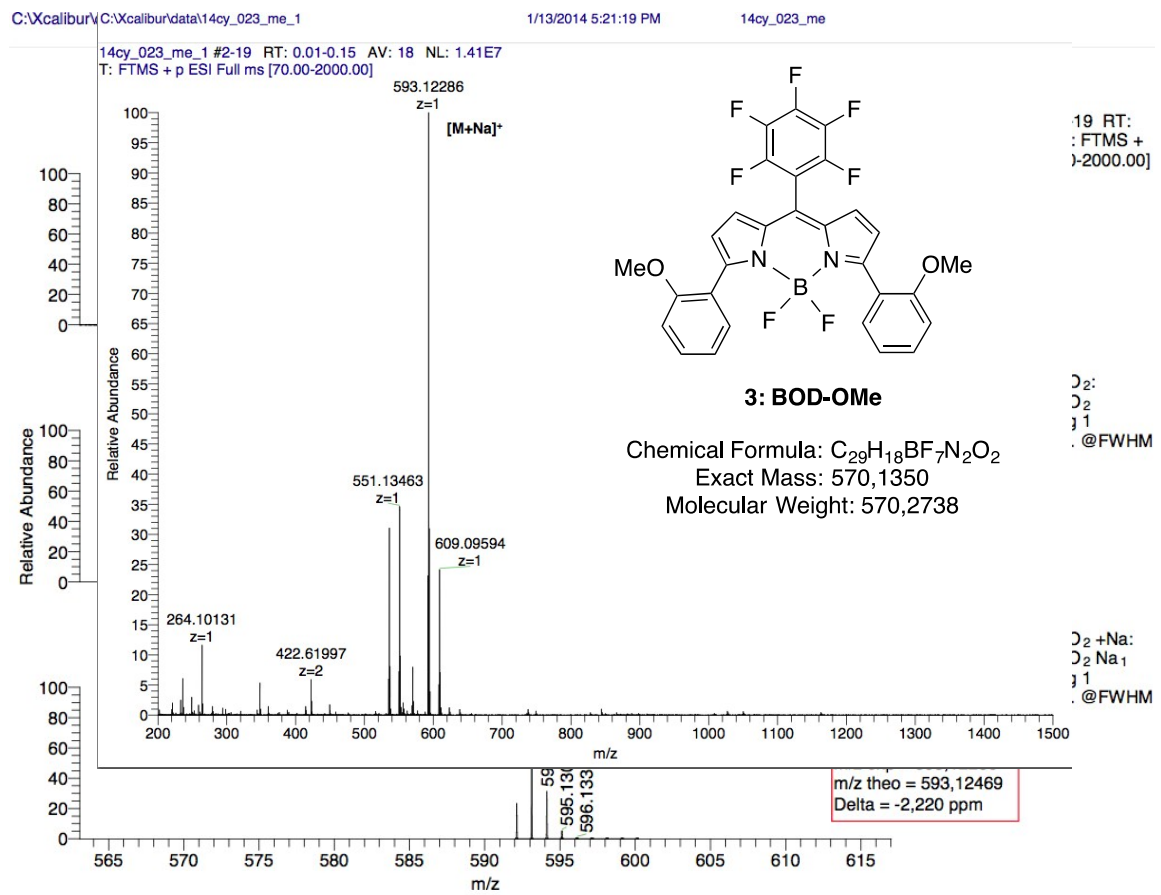
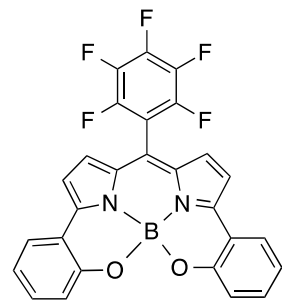
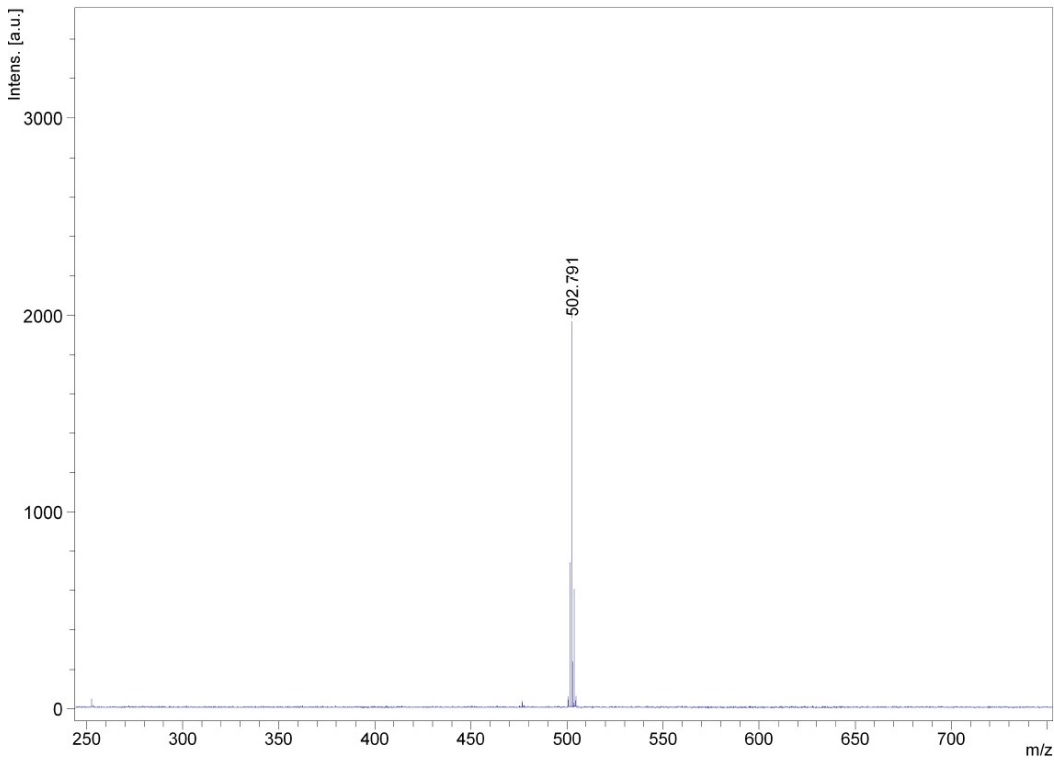


Figure S18. HRMS (ESI) mass spectra of **BOD-OMe** (**3**).



4: BOD-O

Chemical Formula: $C_{27}H_{12}BF_5N_2O_2$
Exact Mass: 502.0912
Molecular Weight: 502.2070

Figure S19. MALDI-TOF mass spectrum of **BOD-O (4)**.

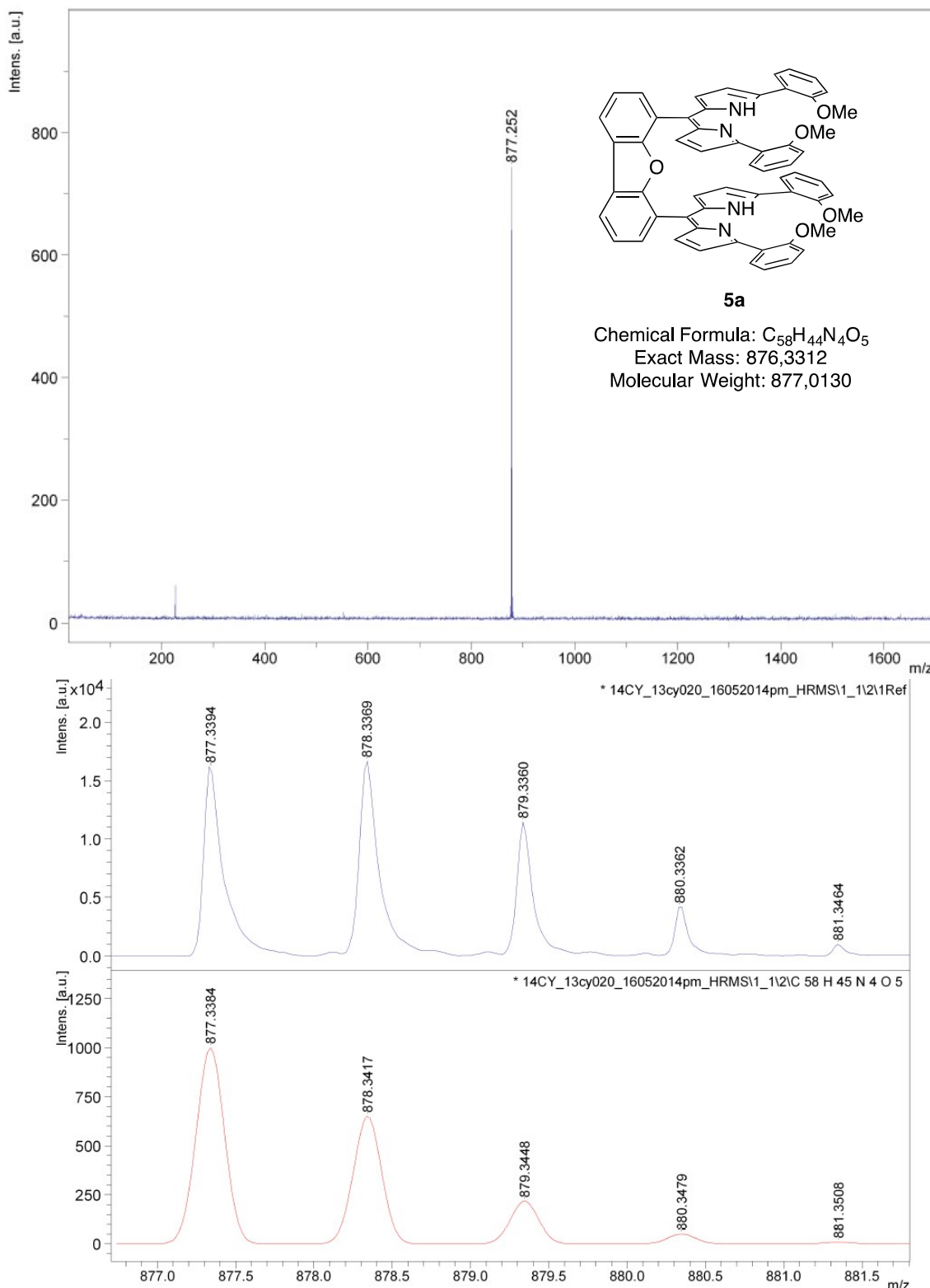
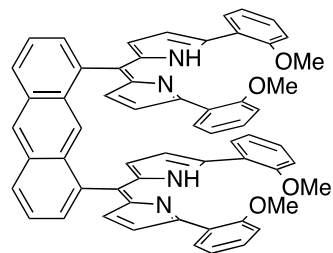
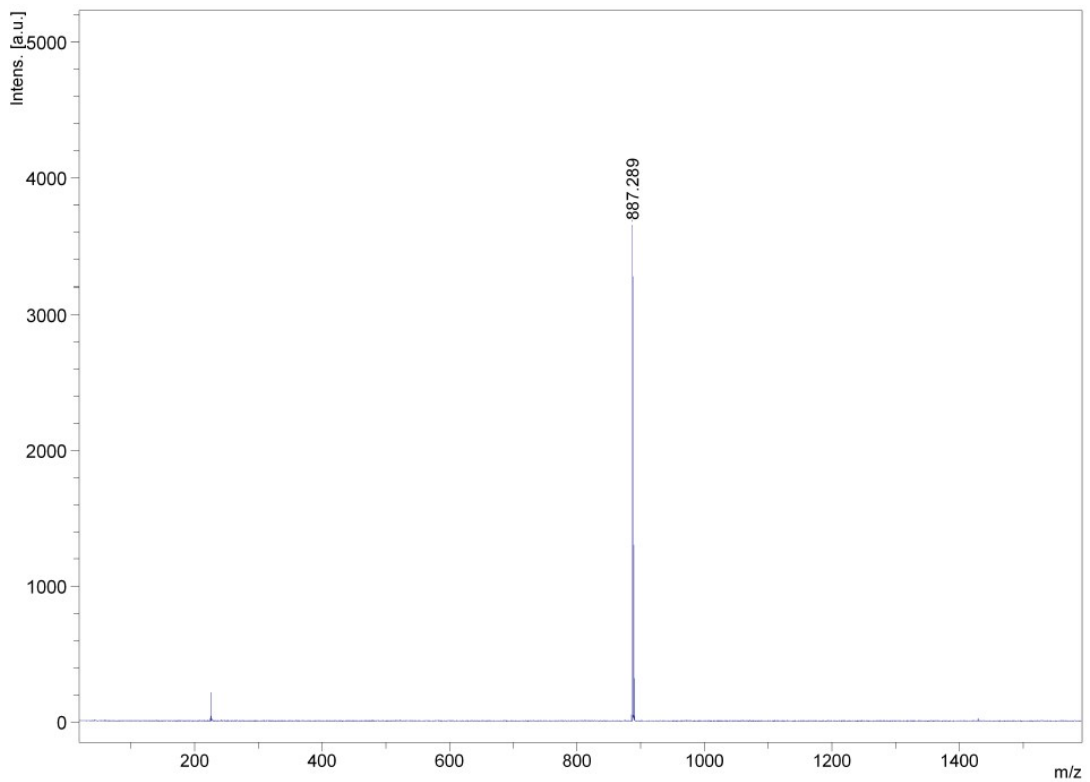


Figure S20. HRMS (MALDI-TOF) mass spectra of **5a**.



6a

Chemical Formula: $C_{60}H_{46}N_4O_4$
Exact Mass: 886.3519
Molecular Weight: 887.0520

Figure S21. MALDI-TOF mass spectrum of **6a**.

14cy_020bdp_me_2 #1-20 RT: 0.00-0.27 AV: 20 NL: 2.89E6
T: FTMS + p ESI Full ms [100.00-2000.00]

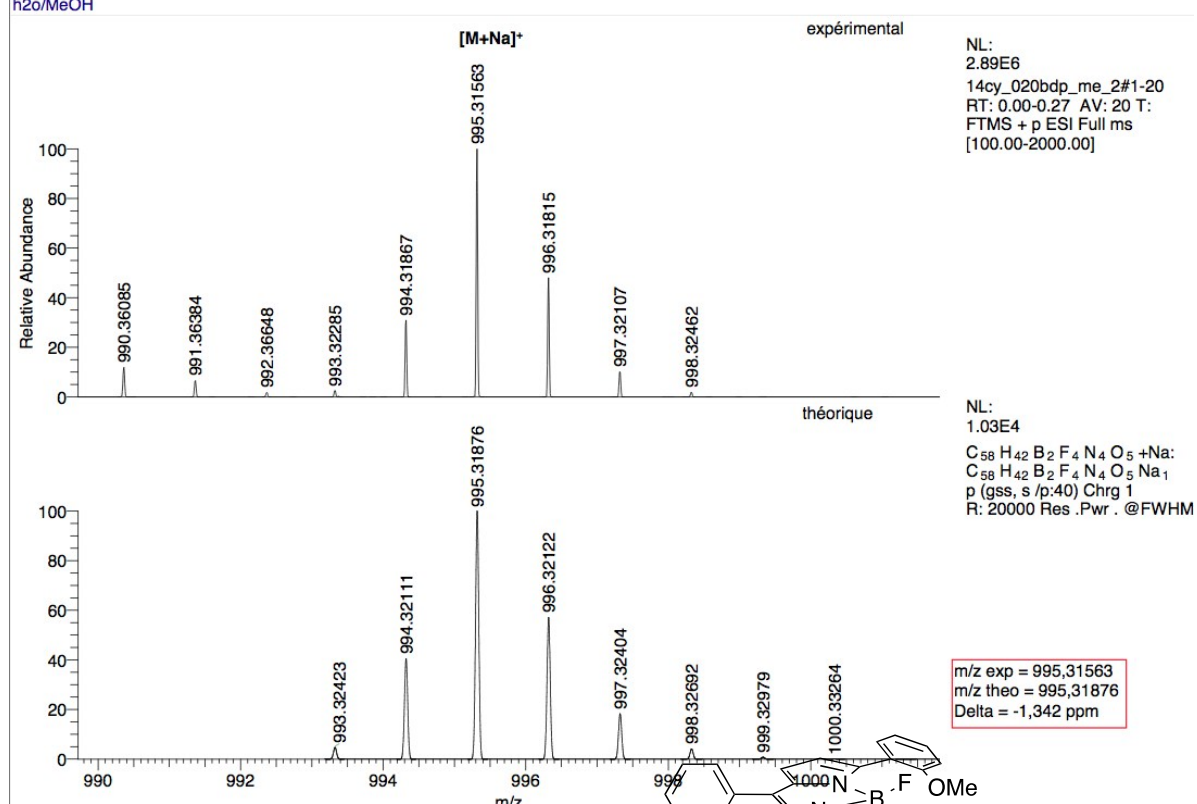
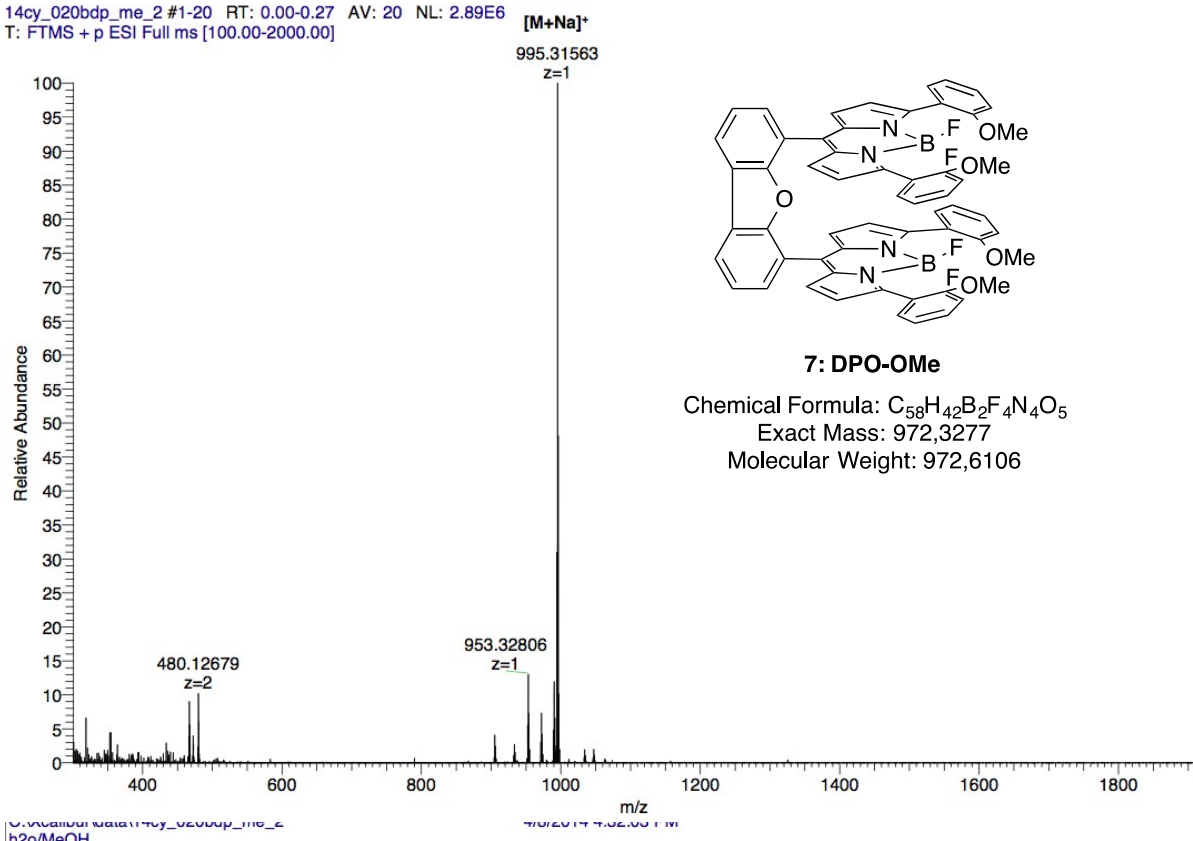
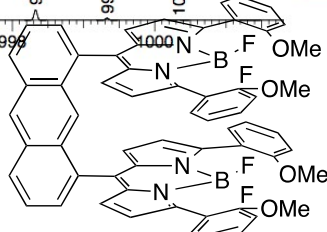


Figure S22. HRMS (ESI) mass spectra of DPO-



S16

8: DPA-OMe

Chemical Formula: $C_{60}H_{44}B_2F_4N_4O_4$
Exact Mass: 982,3485
Molecular Weight: 982,6496

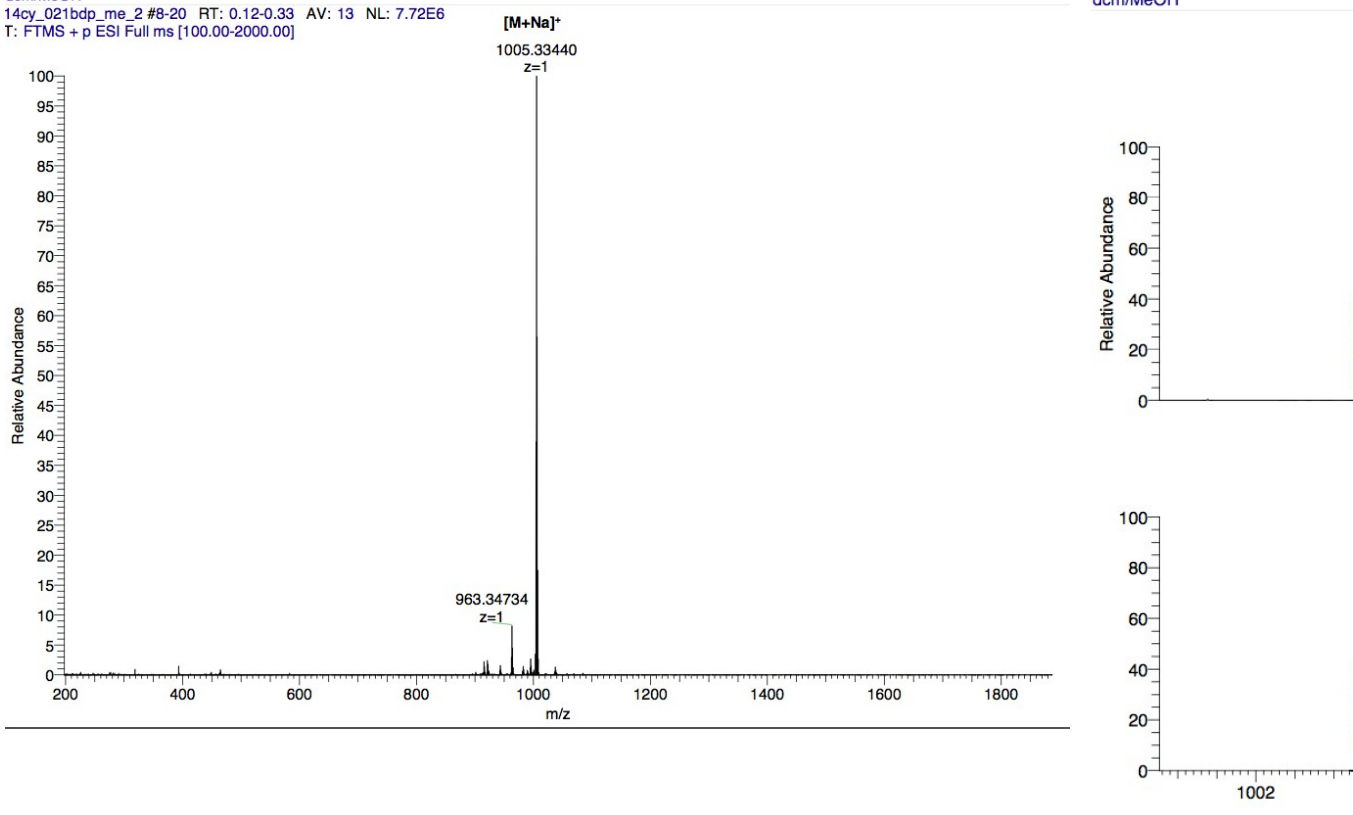
14cy_021bdp_me_2 #8-20 RT: 0.12-0.33 AV: 13 NL: 7.72E6
T: FTMS + p ESI Full ms [100.00-2000.00]

Figure S23. HRMS (ESI) mass spectra of DPA-OMe (**8**).

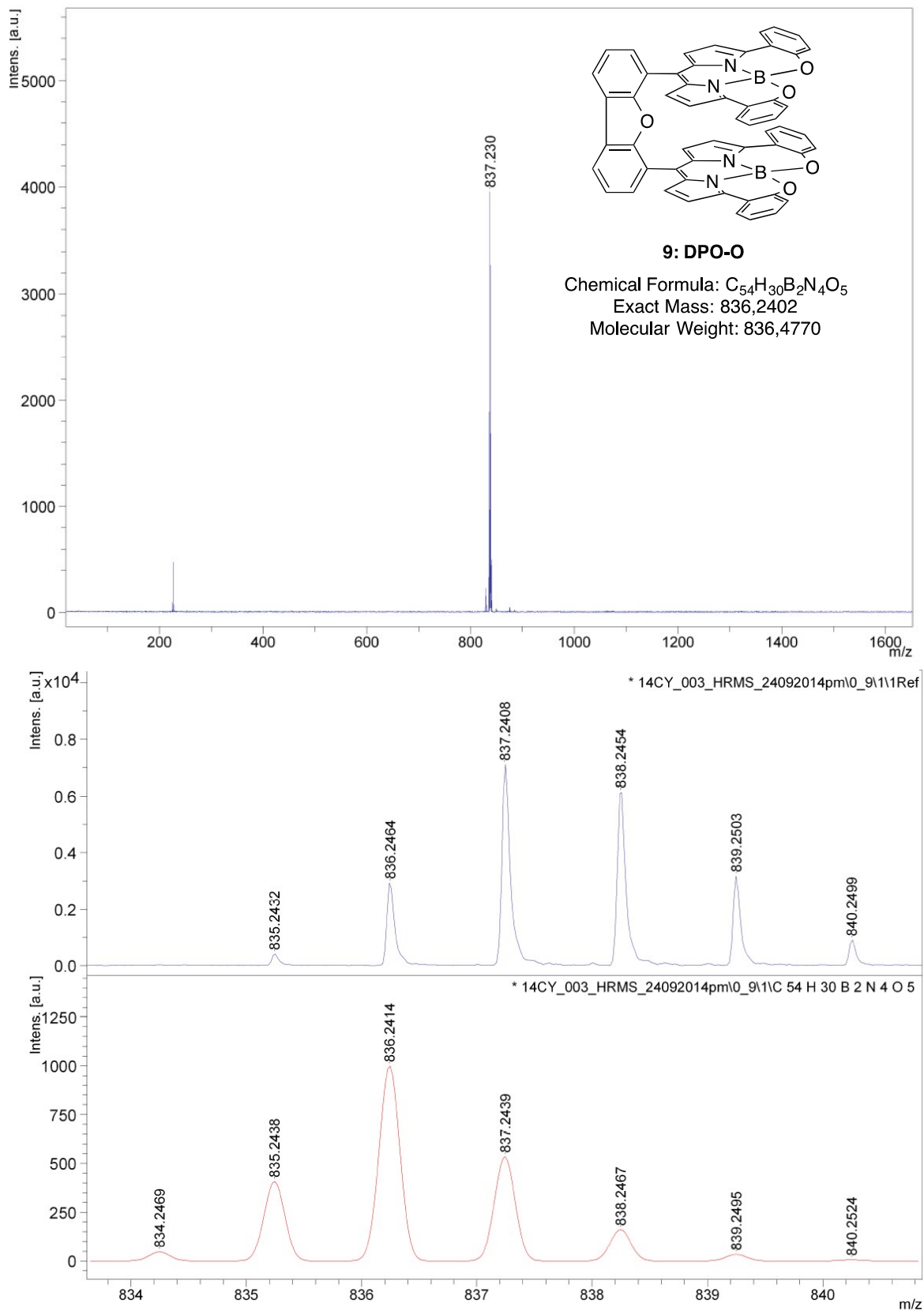


Figure S24. HRMS (MALDI-TOF) mass spectra of DPO-O (**9**).

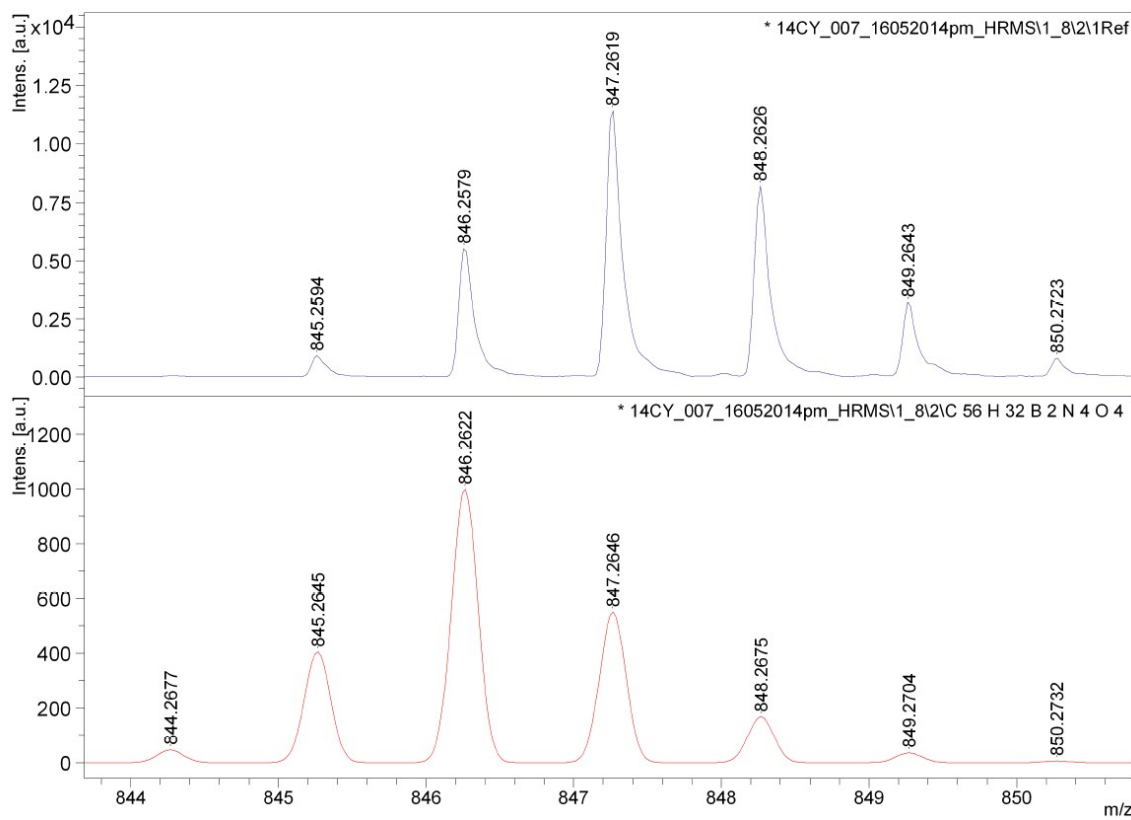
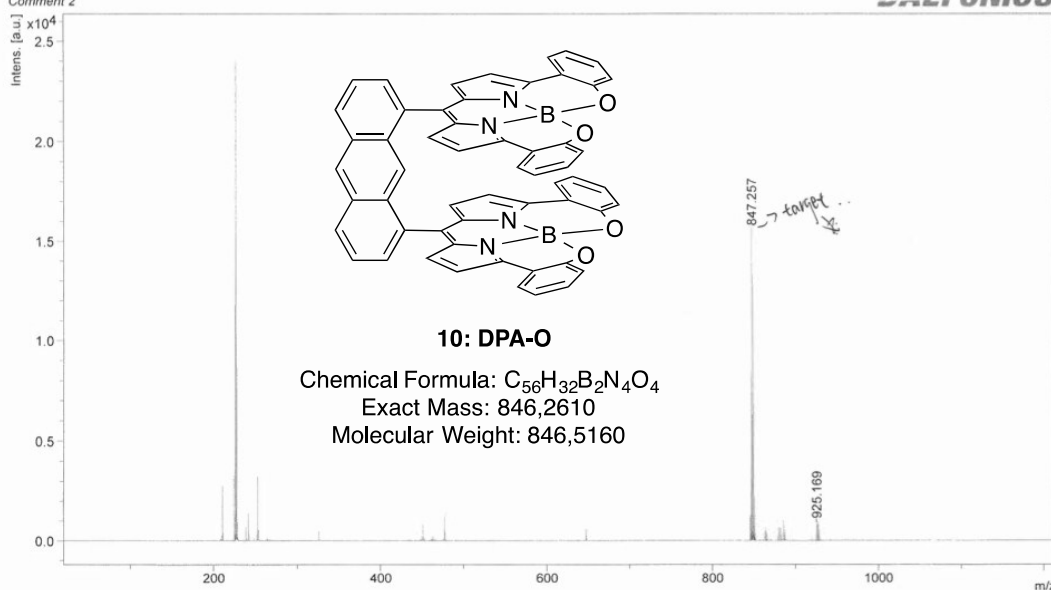


Figure S25. HRMS (MALDI/TOF) mass spectra of **DPA-O (10)**.

Calculation Procedure

All density functional theory (DFT) and time dependent density functional theory (TD-DFT) calculations were performed with Gaussian 09 [1] at the Université de Sherbrooke with the Mammouth supercomputer supported by *Le Réseau Québécois De Calculs Hautes Performances*. The DFT geometry optimisations as well as TD-DFT calculations [2-11] were carried out using the B3LYP method. A 6-31g* basis set was applied to all atoms [12-17]. All calculations were carried out in a THF solvent field. The calculated absorption spectra were obtained from GaussSum 2.1 [18].

1. Frisch MJ *et al.* *Gaussian, Inc., Wallingford CT*, 2004.
2. Hohenberg P and Kohn W. *Phys. Rev.* 1964; **136**: B864–871.
3. Hohenberg P and Kohn W. *J. Phys. Rev.* 1965; **140**: A1133–1138.
4. Parr RG and Yang W. *Density-functional theory of atoms and molecules*, Oxford Univ. Press: Oxford, 1989.
5. Salahub DR and Zerner MC. *The Challenge of d and f Electrons*, Amer. Chem. Soc. Washington, D.C. 1989.
6. Bauernschmitt R and Ahlrichs R. *Chem. Phys. Lett.* 1996; **256**: 454–464.
7. Casida ME, Jamorski C, Casida KC and Salahub DR. *J. Chem. Phys.* 1998; **108**: 4439–4449.
8. Stratmann RE, Scuseria GE and Frisch MJ. *J. Chem. Phys.* 1998; **109**: 8218–8224.
9. Lee C, Yang W and Parr RG. *Phys. Rev. B* 1988; **37**: 785–789.
10. Miehlich B, Savin A, Stoll H and Preuss H. *Chem. Phys. Lett.* 1989; **157**: 200–206.
11. Becke AD. *J. Chem. Phys.* 1993; **98**: 5648–5652.
12. Binkley JS, Pople JA and Hehre WJ. *J. Am. Chem. Soc.* 1980; **102**: 939–947.
13. Gordon MS, Binkley JS, Pople JA, Pietro WJ and Hehre WJ. *J. Am. Chem. Soc.* 1982; **104**: 2797–2803.
14. Pietro WJ, Franci MM, Hehre WJ, Defrees DJ, Pople JA and Binkley JS. *J. Am. Chem. Soc.* 1982; **104**: 5039–5048.
15. Dobbs KD and Hehre WJ. *J. Comput. Chem.* 1986; **7**: 359–378.
16. Dobbs KD and Hehre WJ. *J. Comput. Chem.* 1987; **8**: 861–879.
17. Dobbs KD and Hehre WJ. *J. Comput. Chem.* 1987; **8**: 880–893.
18. O’Boyle NM, Tenderholt AL and Langner KM. *J. Comp. Chem.* 2008; **29**: 839–845.

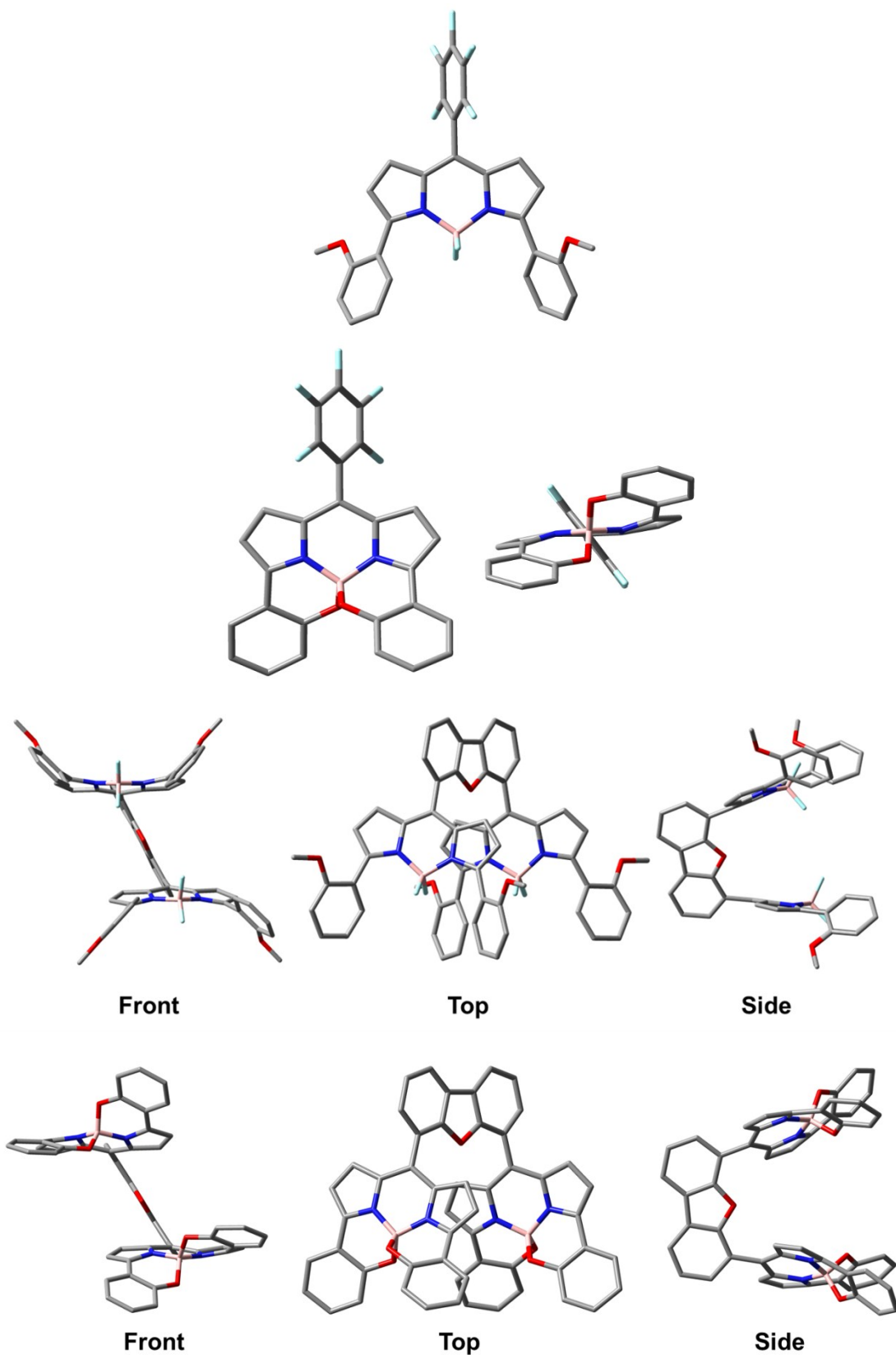


Figure S26. Optimized geometries (DFT, B3LYP) for **BOD-OMe (3)** (first) **BOD-O (4)** (second), **DPO-OMe (7)** (third) and **DPO-O (9)** (fourth).

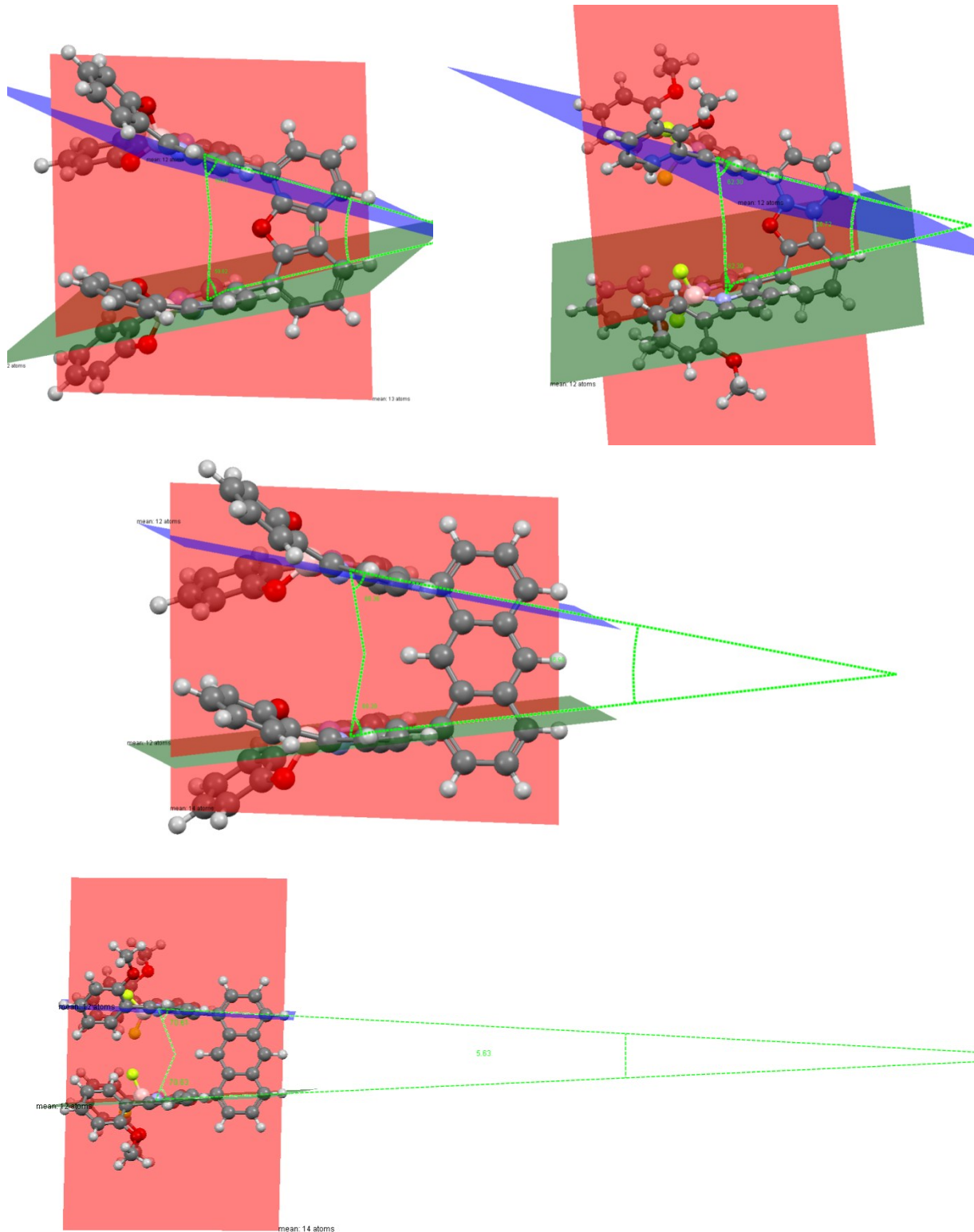


Figure S27. Optimized geometries (DFT, B3LYP) for **DPO-O (9)** (top, left), **DPO-OMe (7)** (top, right), **DPA-O (10)** (middle) and **DPA-OMe (8)** (bottom) showing select structural parameters.

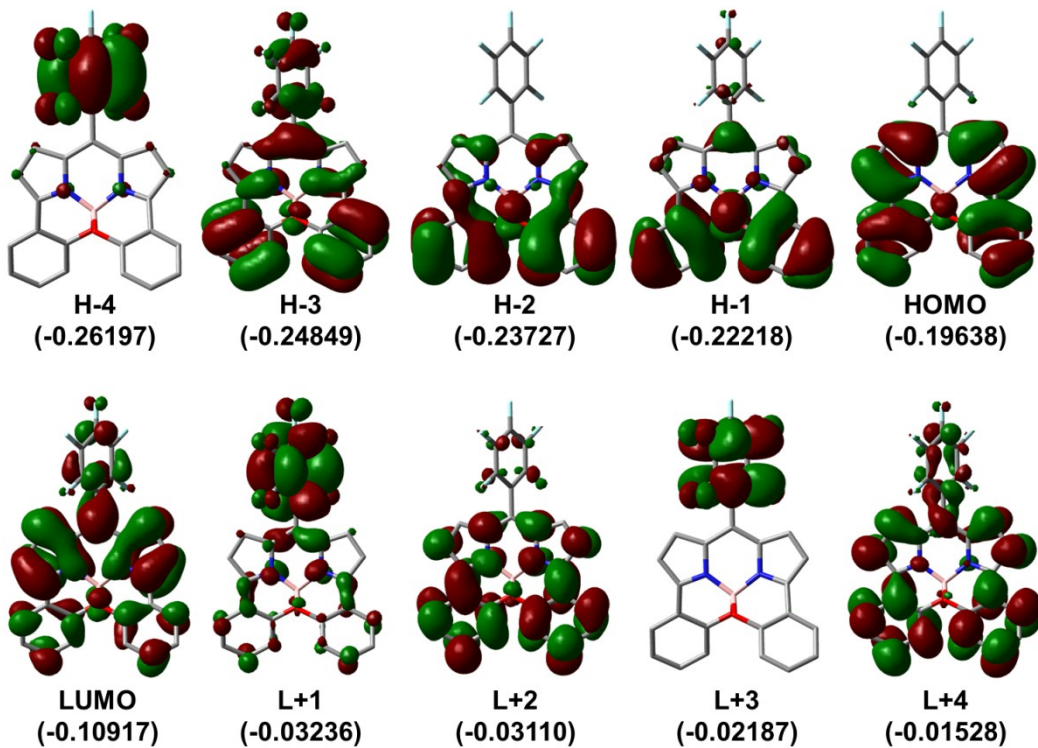


Figure S28. Representations of the frontier MOs for **BOD-O (4)**. The energies are in a.u.

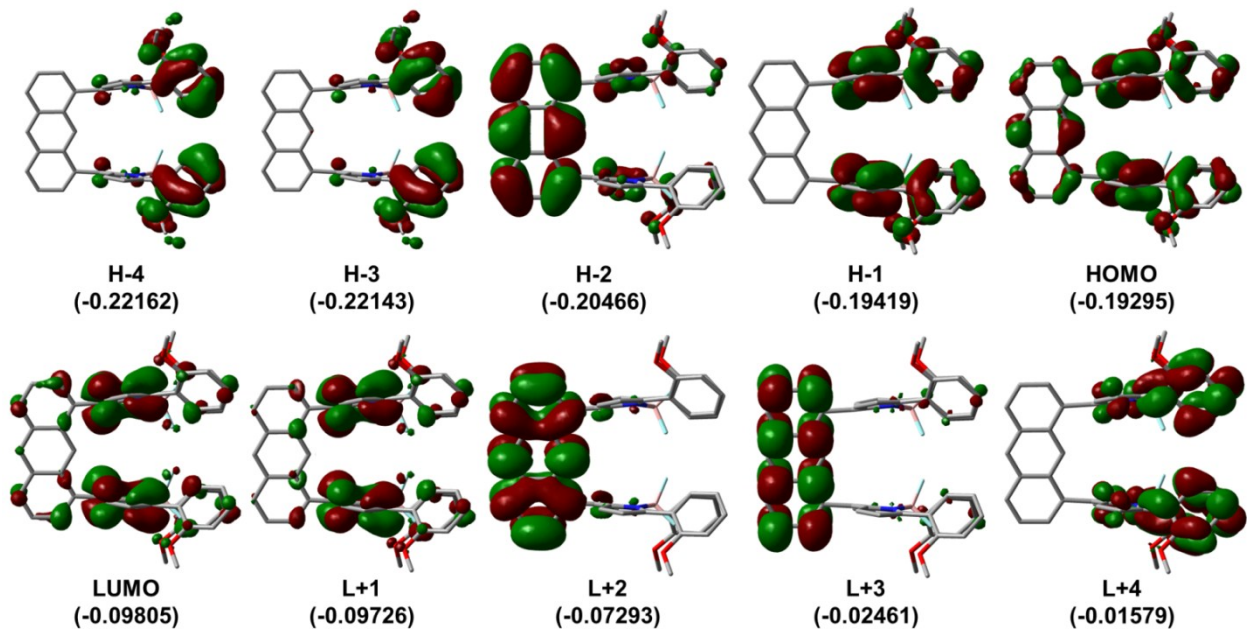


Figure S29. Representations of the frontier MOs for **DPA-OMe (8)**. The energies are in a.u.

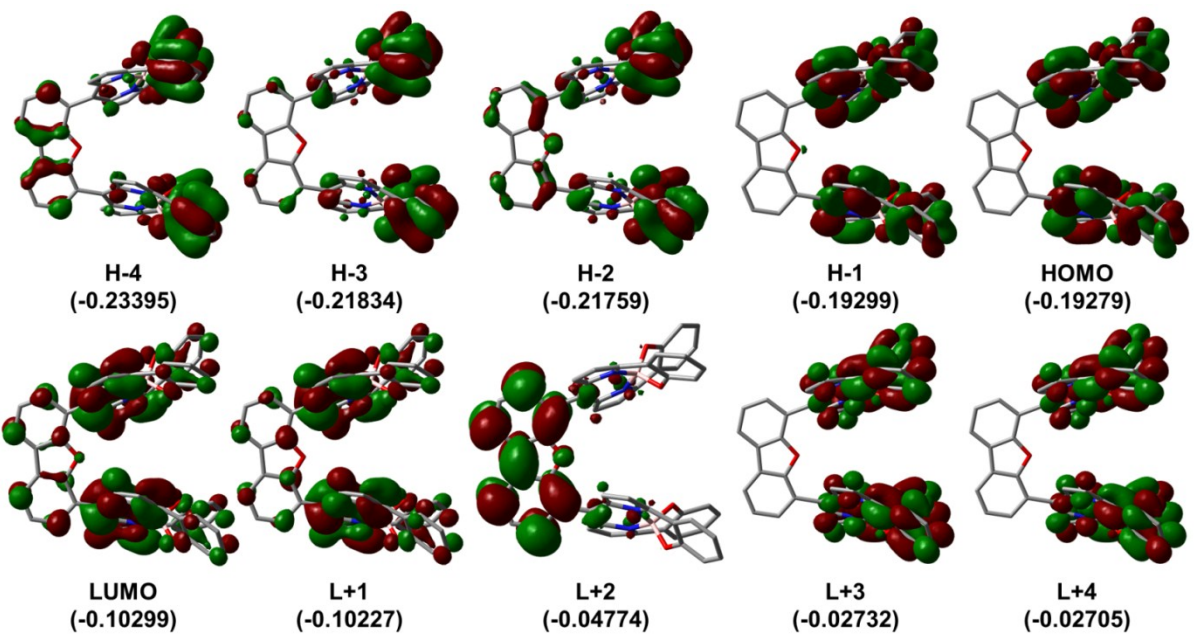


Figure S30. Representations of the frontier MOs for **DPO-O (9)**. The energies are in a.u.

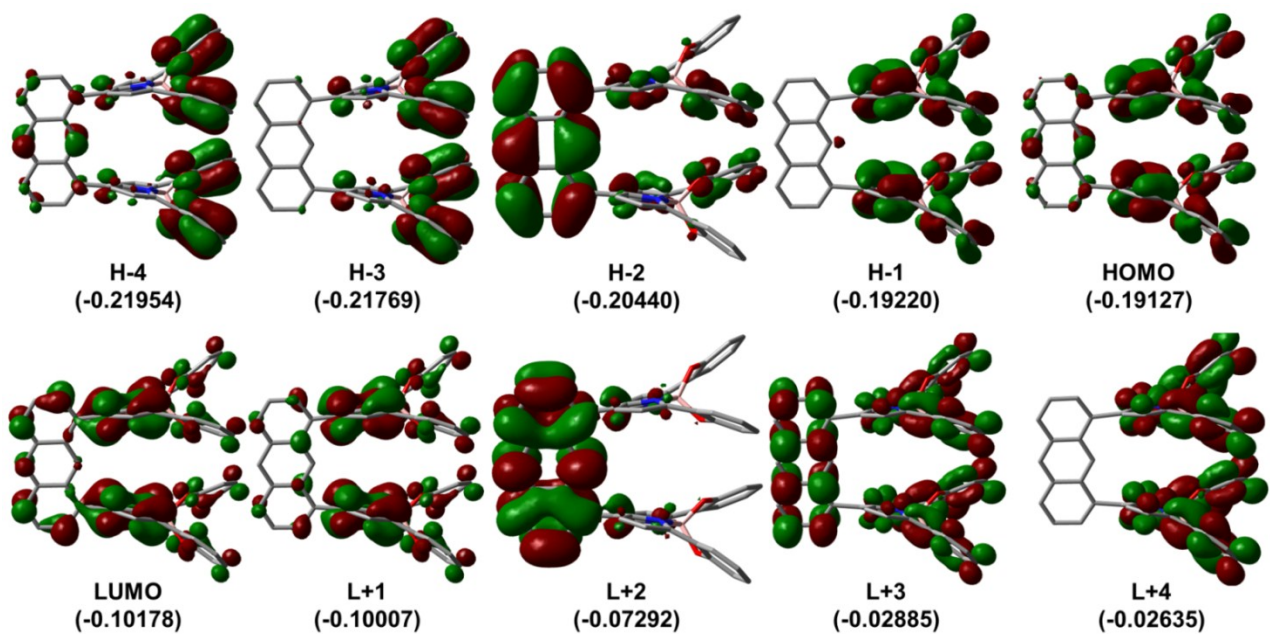


Figure S31. Representations of the frontier MOs for **DPA-O (10)**. The energies are in a.u.

Table 1. Percent distribution of the molecular orbitals over selected molecular fragments of **DPA-OMe (8)**.

| Molecular Fragment | H-4 | H-3 | H-2 | H-1 | HOMO | LUMO | L+1 | L+2 | L+3 | L+4 |
|--------------------|-------------|-------------|-------------|-------------|-------------|-------------|-------------|-------------|-------------|-------------|
| Anthracene | 0.9 | 1.5 | 77.6 | 1.9 | 12.6 | 13.3 | 7.9 | 92.0 | 88.7 | 1.2 |
| BODIPY 1 | 49.4 | 49.4 | 11.2 | 49.1 | 43.6 | 43.2 | 46.2 | 4.0 | 5.7 | 49.2 |
| BODIPY 2 | 49.6 | 49.2 | 11.2 | 49.0 | 43.8 | 43.5 | 45.9 | 4.0 | 5.7 | 49.6 |

Table 2. Percent distribution of the molecular orbitals over selected molecular fragments of **DPO-O (9)**.

| Molecular Fragment | H-4 | H-3 | H-2 | H-1 | HOMO | LUMO | L+1 | L+2 | L+3 | L+4 |
|--------------------|-------------|-------------|-------------|-------------|-------------|-------------|-------------|-------------|-------------|-------------|
| Dibenzofuran | 9.3 | 3.9 | 8.6 | 2.9 | 5.0 | 12.7 | 10.1 | 86.0 | 1.9 | 3.8 |
| BODIPY 1 | 45.1 | 48.1 | 45.7 | 48.6 | 47.4 | 43.6 | 45.0 | 7.0 | 49.1 | 48.0 |
| BODIPY 2 | 45.6 | 48.0 | 45.7 | 48.5 | 47.5 | 43.6 | 45.0 | 7.0 | 49.0 | 48.1 |

Table 3. Percent distribution of the molecular orbitals over selected molecular fragments of **DPA-O (10)**.

| Molecular Fragment | H-4 | H-3 | H-2 | H-1 | HOMO | LUMO | L+1 | L+2 | L+3 | L+4 |
|--------------------|-------------|-------------|-------------|-------------|-------------|-------------|-------------|-------------|-------------|-------------|
| Anthracene | 7.8 | 2.2 | 72.8 | 3.9 | 9.1 | 17.8 | 9.0 | 86.9 | 43.2 | 3.0 |
| BODIPY 1 | 46.1 | 48.9 | 13.6 | 48.0 | 45.5 | 41.1 | 45.5 | 6.6 | 28.4 | 48.5 |
| BODIPY 2 | 46.1 | 48.9 | 13.6 | 48.0 | 45.5 | 41.1 | 45.5 | 6.6 | 28.4 | 48.5 |

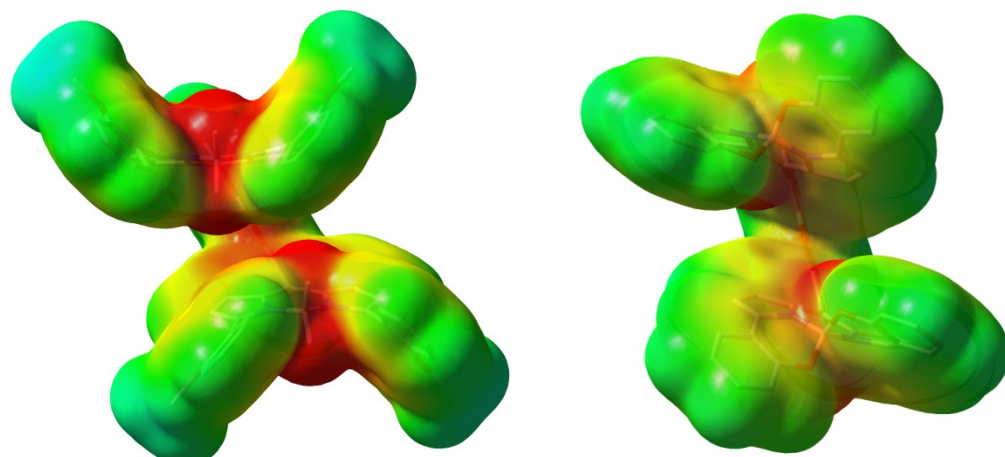


Figure S32. Electronic density map (DFT) for **DPA-OMe (8)** and **DPA-O (10)**. The red and blue areas are respectively the electron rich and poor segments of the molecule.

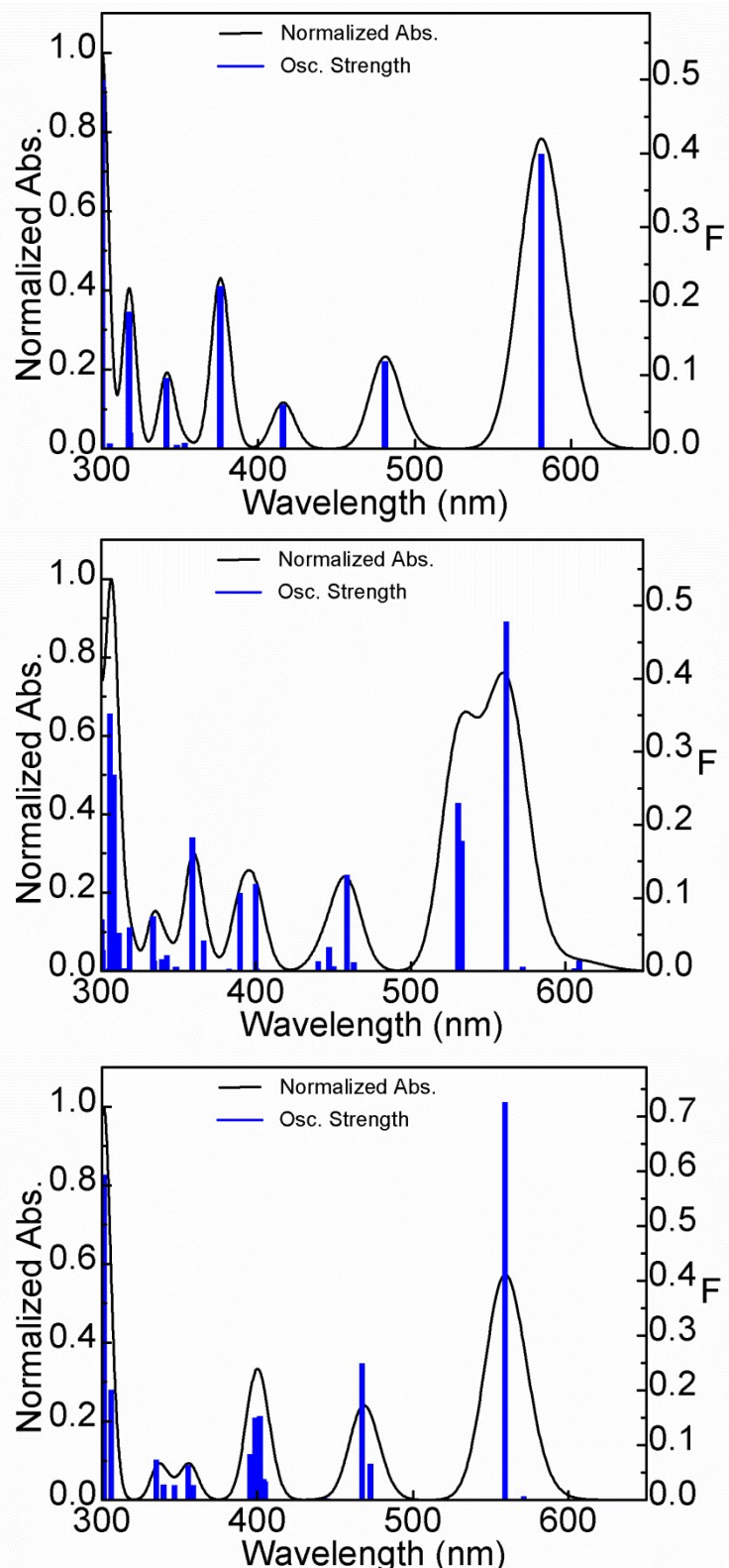


Figure S33. Graphs reported the computed oscillator strength (F) as a function of the calculated positions of the first 75 electronic transitions for **BOD-O (4)** (top), **DPA-O (10)** (middle) and **DPO-O (9)** (bottom).

Table 4. Computed oscillator strengths (F), positions of the first electronic transitions and major contributions of **BOD-OMe (3)**.

| Transition No. | Wavelength (nm) | Osc. Strength | Major contributors (%) |
|----------------|-----------------|---------------|--|
| 1 | 533.5 | 0.6403 | HOMO→LUMO (96) |
| 2 | 452.8 | 0.0826 | H-1→LUMO (99) |
| 3 | 421.0 | 0.0845 | H-2→LUMO (95) |
| 4 | 362.9 | 0.0483 | H-4→LUMO (77), H-3→LUMO (21) |
| 5 | 359.1 | 0.1597 | H-4→LUMO (21), H-3→LUMO (75) |
| 6 | 346.9 | 0.0013 | H-5→LUMO (99) |
| 7 | 337.4 | 0.0443 | H-6→LUMO (94) |
| 8 | 323.7 | 0.035 | H-8→LUMO (94) |
| 9 | 318.7 | 0.0469 | H-7→LUMO (86) |
| 10 | 313.0 | 0.0168 | HOMO→L+1 (98) |
| 11 | 288.4 | 0.151 | HOMO→L+2 (92) |
| 12 | 279.1 | 0.2537 | HOMO→L+3 (91) |
| 13 | 266.6 | 0.0039 | HOMO→L+4 (91) |
| 14 | 256.0 | 0.0062 | H-1→L+1 (93) |
| 15 | 253.6 | 0.0135 | H-1→L+2 (30), H-1→L+3 (16), HOMO→L+6 (21) |
| 16 | 252.8 | 0.0155 | H-9→LUMO (11), H-2→L+2 (12), H-1→L+4 (15), HOMO→L+5 (31) |
| 17 | 246.5 | 0.0078 | H-2→L+1 (94) |
| 18 | 245.4 | 0.2013 | H-9→LUMO (66) |
| 19 | 240.8 | 0.0275 | H-1→L+2 (47), HOMO→L+6 (27) |
| 20 | 240.7 | 0.0044 | HOMO→L+7 (89) |
| 21 | 237.7 | 0.0369 | H-5→L+1 (13), H-1→L+3 (42), HOMO→L+6 (33) |
| 22 | 236.6 | 0.0021 | H-10→LUMO (13), H-2→L+2 (26), HOMO→L+5 (36) |
| 23 | 235.4 | 0.0147 | H-12→LUMO (20), H-10→LUMO (40), H-2→L+2 (11) |
| 24 | 234.1 | 0.0263 | H-8→L+2 (11), H-5→L+1 (43), H-1→L+3 (21) |
| 25 | 231.9 | 0.0161 | H-2→L+2 (37), H-1→L+4 (51) |
| 26 | 229.9 | 0.0007 | H-11→LUMO (83), H-10→LUMO (12) |
| 27 | 229.3 | 0.0244 | H-12→LUMO (27), H-10→LUMO (12), H-2→L+3 (33) |
| 28 | 228.9 | 0.0016 | H-13→LUMO (17), H-12→LUMO (20), H-2→L+3 (38), H-1→L+4 (10) |
| 29 | 227.9 | 0.0071 | H-13→LUMO (72), H-12→LUMO (10) |
| 30 | 226.2 | 0.0252 | H-2→L+4 (70) |
| 31 | 225.3 | 0.0026 | H-4→L+1 (74), H-3→L+1 (19) |
| 32 | 224.2 | 0.0041 | H-4→L+1 (19), H-3→L+1 (76) |
| 33 | 221.3 | 0.0002 | H-14→LUMO (83), H-12→LUMO (10) |
| 34 | 217.6 | 0.0136 | H-6→L+1 (95) |
| 35 | 216.1 | 0.0144 | H-3→L+2 (47), H-3→L+3 (13), H-1→L+5 (21) |
| 36 | 213.5 | 0.0063 | H-4→L+2 (73), HOMO→L+8 (15) |
| 37 | 212.7 | 0.0261 | H-3→L+4 (13), H-1→L+6 (29), HOMO→L+8 (28) |
| 38 | 210.1 | 0.0379 | H-4→L+3 (25), H-3→L+2 (21), H-3→L+3 (25) |
| 39 | 209.8 | 0.0603 | H-4→L+3 (26), H-3→L+2 (15), H-3→L+3 (11) |

| | | | |
|----|-------|--------|--|
| 40 | 209.3 | 0.0106 | H-15→LUMO (67) |
| 41 | 208.8 | 0.0024 | H-7→L+1 (82) |
| 42 | 207.9 | 0.1781 | H-4→L+3 (35), H-1→L+6 (17), HOMO→L+8 (18) |
| 43 | 207.7 | 0.0421 | H-16→LUMO (18), H-6→L+2 (45), H-4→L+4 (15) |
| 44 | 207.1 | 0.0028 | H-1→L+7 (90) |
| 45 | 206.6 | 0.0343 | H-16→LUMO (18), H-3→L+3 (18), H-2→L+6 (10), H-1→L+5 (31) |
| 46 | 206.3 | 0.0119 | H-16→LUMO (47), H-15→LUMO (12) |
| 47 | 205.6 | 0.0124 | H-5→L+2 (31), H-5→L+7 (50) |
| 48 | 204.6 | 0.0174 | H-2→L+5 (56), H-1→L+6 (18) |
| 49 | 204.0 | 0.0065 | H-6→L+2 (21), H-6→L+3 (42), H-4→L+4 (17) |
| 50 | 203.9 | 0.003 | H-17→LUMO (14), H-8→L+1 (29), H-5→L+2 (13), H-5→L+7 (16) |
| 51 | 201.9 | 0.0111 | H-17→LUMO (45), H-7→L+2 (16), H-3→L+4 (14) |
| 52 | 201.7 | 0.1402 | H-17→LUMO (24), H-7→L+2 (17), H-3→L+4 (17) |
| 53 | 201.6 | 0.0326 | H-6→L+3 (16), H-4→L+4 (11), H-2→L+6 (43) |
| 54 | 200.7 | 0.005 | H-5→L+2 (10), H-5→L+3 (20), H-2→L+7 (43) |
| 55 | 200.6 | 0.0076 | H-19→LUMO (42), H-18→LUMO (11), H-2→L+7 (28) |
| 56 | 200.2 | 0.0252 | H-19→LUMO (10), H-5→L+3 (31), H-2→L+7 (23) |
| 57 | 198.8 | 0.0415 | H-6→L+3 (16), H-4→L+4 (30) |
| 58 | 198.0 | 0.0496 | H-19→LUMO (18), H-18→LUMO (54) |
| 59 | 196.9 | 0.0274 | H-7→L+2 (34), H-7→L+3 (39) |
| 60 | 196.7 | 0.0159 | H-8→L+7 (35), H-3→L+7 (11) |
| 61 | 196.0 | 0.0239 | H-8→L+7 (16), HOMO→L+9 (47) |
| 62 | 194.7 | 0.0726 | H-6→L+4 (80) |
| 63 | 193.7 | 0.0004 | H-5→L+4 (97) |
| 64 | 193.1 | 0.0008 | H-8→L+2 (35), H-8→L+3 (29), H-8→L+7 (10) |
| 65 | 191.4 | 0.0228 | H-20→LUMO (17), H-1→L+8 (28) |
| 66 | 190.9 | 0.0387 | H-7→L+3 (10), H-3→L+5 (10), H-1→L+8 (30) |
| 67 | 190.6 | 0.0319 | H-20→LUMO (63), H-7→L+4 (11) |
| 68 | 188.5 | 0.0643 | H-21→LUMO (11), H-4→L+5 (40) |
| 69 | 188.3 | 0.0036 | H-26→LUMO (11), H-21→LUMO (48), H-4→L+5 (16) |
| 70 | 187.6 | 0.0031 | H-9→L+1 (11), H-4→L+5 (12), H-4→L+6 (10), H-3→L+5 (10) |
| 71 | 187.1 | 0.035 | H-6→L+5 (11), H-4→L+6 (54) |
| 72 | 186.4 | 0.0463 | H-22→LUMO (63) |
| 73 | 185.8 | 0.0212 | H-9→L+1 (19), H-8→L+4 (52) |
| 74 | 185.6 | 0.0873 | H-7→L+4 (36) |
| 75 | 185.5 | 0.2365 | H-9→L+1 (11), H-3→L+6 (15) |

Table 5. Computed oscillator strengths (F), positions of the first electronic transitions and major contributions of **BOD-O (4)**.

| Transition No. | Wavelength (nm) | Osc. Strength | Major contributors (%) |
|----------------|-----------------|---------------|--|
| 1 | 580.8 | 0.3993 | HOMO→LUMO (99) |
| 2 | 480.9 | 0.1187 | H-1→LUMO (98) |
| 3 | 415.8 | 0.0594 | H-2→LUMO (98) |
| 4 | 375.7 | 0.2197 | H-3→LUMO (92) |
| 5 | 353.0 | 0.0076 | H-5→LUMO (84), H-4→LUMO (15) |
| 6 | 348.1 | 0.0047 | H-5→LUMO (15), H-4→LUMO (84) |
| 7 | 341.3 | 0.0954 | H-6→LUMO (90) |
| 8 | 318.0 | 0.0212 | HOMO→L+1 (99) |
| 9 | 317.3 | 0.1853 | H-7→LUMO (81), HOMO→L+2 (17) |
| 10 | 305.1 | 0.0068 | H-8→LUMO (85), HOMO→L+4 (13) |
| 11 | 300.2 | 0.4992 | H-7→LUMO (15), HOMO→L+2 (72) |
| 12 | 293.1 | 0.0458 | HOMO→L+3 (94) |
| 13 | 276.1 | 0.0326 | H-8→LUMO (10), HOMO→L+4 (82) |
| 14 | 272.3 | 0.0725 | H-1→L+2 (79), HOMO→L+6 (14) |
| 15 | 264.4 | 0.0114 | H-1→L+1 (67), HOMO→L+5 (16) |
| 16 | 258.4 | 0.0014 | H-9→LUMO (97) |
| 17 | 257.2 | 0.0005 | H-2→L+2 (19), H-1→L+1 (30), HOMO→L+5 (36) |
| 18 | 251.1 | 0.004 | H-11→LUMO (58), H-10→LUMO (35) |
| 19 | 247.9 | 0.1228 | H-1→L+2 (13), H-1→L+3 (15), HOMO→L+6 (55) |
| 20 | 246.7 | 0.0361 | H-1→L+3 (72), HOMO→L+6 (14) |
| 21 | 245.4 | 0.0002 | HOMO→L+7 (92) |
| 22 | 243.9 | 0.0852 | H-2→L+2 (25), H-1→L+4 (56) |
| 23 | 241.6 | 0.0006 | H-2→L+2 (40), HOMO→L+5 (38) |
| 24 | 239.4 | 0.0437 | H-2→L+1 (89) |
| 25 | 238.8 | 0.0347 | H-11→LUMO (24), H-10→LUMO (51), H-1→L+4 (12) |
| 26 | 233.2 | 0.0056 | H-7→L+3 (15), H-4→L+1 (46), H-3→L+3 (20), H-1→L+3 (11) |
| 27 | 232.3 | 0.0122 | H-12→LUMO (92) |
| 28 | 229.0 | 0.0171 | H-3→L+2 (70), H-1→L+5 (12) |
| 29 | 227.8 | 0.0178 | H-3→L+1 (87) |
| 30 | 225.8 | 0.0001 | H-2→L+3 (99) |
| 31 | 225.0 | 0.0184 | H-3→L+2 (11), H-2→L+4 (77) |
| 32 | 219.9 | 0.02 | H-5→L+2 (28), HOMO→L+8 (51) |
| 33 | 217.8 | 0.2032 | H-1→L+5 (71) |
| 34 | 217.5 | 0.0017 | H-5→L+2 (11), H-3→L+4 (20), H-1→L+6 (53) |
| 35 | 217.3 | 0.0104 | H-5→L+1 (95) |
| 36 | 214.5 | 0.0105 | H-6→L+1 (91) |
| 37 | 213.8 | 0.0158 | H-6→L+2 (80) |
| 38 | 212.7 | 0.0065 | H-1→L+7 (87) |
| 39 | 212.2 | 0.0004 | H-4→L+2 (91) |
| 40 | 211.8 | 0.0258 | H-7→L+3 (12), H-4→L+1 (12), H-3→L+3 (71) |

| | | | |
|----|-------|--------|--|
| 41 | 211.3 | 0.0056 | H-5→L+2 (44), H-3→L+4 (25), HOMO→L+8 (12) |
| 42 | 209.9 | 0.0053 | H-13→LUMO (84), H-2→L+6 (11) |
| 43 | 209.8 | 0.1067 | H-3→L+4 (39), H-2→L+5 (18), H-1→L+6 (22) |
| 44 | 205.8 | 0.0002 | H-5→L+3 (93) |
| 45 | 203.7 | 0.0048 | H-14→LUMO (68), H-4→L+7 (10) |
| 46 | 203.5 | 0.0006 | H-6→L+3 (88) |
| 47 | 203.3 | 0.0044 | H-4→L+7 (75) |
| 48 | 203.1 | 0.0251 | H-7→L+2 (34), H-6→L+3 (10), H-2→L+6 (32) |
| 49 | 202.0 | 0.1 | H-8→L+2 (46), H-7→L+1 (11), H-2→L+5 (27) |
| 50 | 201.2 | 0.0262 | H-14→LUMO (11), H-7→L+1 (40), H-4→L+3 (26) |
| 51 | 200.7 | 0.003 | H-8→L+1 (26), H-7→L+2 (32), H-5→L+4 (18) |
| 52 | 199.9 | 0.0541 | H-8→L+1 (21), H-2→L+6 (16), HOMO→L+9 (42) |
| 53 | 199.7 | 0.0558 | H-8→L+1 (33), H-5→L+4 (47) |
| 54 | 198.5 | 0.0326 | H-15→LUMO (36), H-6→L+4 (50) |
| 55 | 197.9 | 0.0062 | H-7→L+7 (11), H-3→L+5 (15), H-3→L+7 (15), H-1→L+8 (29) |
| 56 | 197.9 | 0.0001 | H-4→L+4 (58), H-1→L+8 (15) |
| 57 | 197.7 | 0.0041 | H-7→L+7 (11), H-4→L+4 (27), H-3→L+7 (27), H-1→L+8 (11) |
| 58 | 196.8 | 0.013 | H-2→L+5 (10), H-2→L+7 (67) |
| 59 | 195.9 | 0.1757 | H-15→LUMO (37), H-6→L+4 (28), H-2→L+7 (12) |
| 60 | 195.4 | 0.0116 | H-16→LUMO (72) |
| 61 | 195.0 | 0.0052 | H-3→L+6 (40), H-2→L+7 (18) |
| 62 | 194.8 | 0.1628 | H-16→LUMO (10), H-7→L+2 (11), H-2→L+6 (10), H-1→L+8 (15), HOMO→L+9 (20) |
| 63 | 193.8 | 0.2642 | H-17→LUMO (18), H-8→L+2 (11), H-3→L+6 (16), H-2→L+5 (12), HOMO→L+10 (16) |
| 64 | 192.7 | 0.0025 | H-18→LUMO (80) |
| 65 | 191.5 | 0.003 | H-17→LUMO (68) |
| 66 | 190.7 | 0.0371 | H-3→L+5 (47), H-1→L+8 (10) |
| 67 | 190.1 | 0 | H-8→L+3 (96) |
| 68 | 188.6 | 0.0313 | H-7→L+4 (64), HOMO→L+10 (15) |
| 69 | 186.3 | 0.0766 | H-8→L+4 (27), H-6→L+5 (22), H-5→L+6 (39) |
| 70 | 186.3 | 0.0024 | H-6→L+6 (38), H-5→L+5 (13), HOMO→L+10 (25) |
| 71 | 185.4 | 0.1292 | H-5→L+5 (37), H-3→L+6 (14), H-2→L+8 (26) |
| 72 | 185.4 | 0.139 | H-8→L+4 (52), H-5→L+6 (23) |
| 73 | 183.2 | 0.0493 | H-21→LUMO (21), H-20→LUMO (31), H-19→LUMO (28) |
| 74 | 182.8 | 0.0985 | H-9→L+2 (49), H-7→L+1 (10), H-4→L+3 (11) |
| 75 | 182.2 | 0.1187 | H-7→L+3 (24), H-7→L+7 (31), H-3→L+7 (18) |

Table 6. Computed oscillator strengths (F), positions of the first electronic transitions and major contributions of **DPO-OMe (7)**.

| Transition No. | Wavelength (nm) | Osc. Strength | Major contributors (%) |
|----------------|-----------------|---------------|--|
| 1 | 565.0 | 0.0005 | H-1→LUMO (43), HOMO→LUMO (11), HOMO→L+1 (37) |
| 2 | 565.0 | 0.0022 | H-1→LUMO (11), H-1→L+1 (37), HOMO→LUMO (43) |
| 3 | 534.9 | 0.0213 | H-1→LUMO (45), HOMO→L+1 (53) |
| 4 | 525.0 | 1.1673 | H-1→L+1 (53), HOMO→LUMO (45) |
| 5 | 438.5 | 0.1145 | H-3→LUMO (46), H-2→L+1 (53) |
| 6 | 435.1 | 0.169 | H-3→L+1 (41), H-2→LUMO (58) |
| 7 | 413.5 | 0.0018 | H-3→LUMO (52), H-2→L+1 (42) |
| 8 | 413.3 | 0.0007 | H-3→L+1 (56), H-2→LUMO (39) |
| 9 | 409.1 | 0.0064 | H-5→LUMO (50), H-4→L+1 (47) |
| 10 | 408.5 | 0.0661 | H-5→L+1 (43), H-4→LUMO (52) |
| 11 | 396.9 | 0.0093 | H-6→LUMO (86) |
| 12 | 395.9 | 0.0211 | H-6→L+1 (81) |
| 13 | 393.6 | 0.0299 | H-7→L+1 (73), H-5→L+1 (10), H-4→LUMO (10) |
| 14 | 392.3 | 0.0875 | H-7→LUMO (77) |
| 15 | 384.9 | 0.0045 | H-7→L+1 (14), H-6→LUMO (11), H-5→L+1 (39), H-4→LUMO (32) |
| 16 | 384.7 | 0.0056 | H-7→LUMO (16), H-6→L+1 (12), H-5→LUMO (33), H-4→L+1 (35) |
| 17 | 357.4 | 0.0028 | H-11→L+1 (45), H-10→LUMO (50) |
| 18 | 357.2 | 0.0681 | H-11→LUMO (48), H-10→L+1 (44) |
| 19 | 351.6 | 0.0251 | HOMO→L+2 (95) |
| 20 | 351.4 | 0.0009 | H-1→L+2 (96) |
| 21 | 347.5 | 0.0302 | H-9→L+1 (19), H-8→LUMO (74) |
| 22 | 345.3 | 0.1732 | H-9→LUMO (23), H-8→L+1 (67) |
| 23 | 334.3 | 0.0012 | H-9→LUMO (66), H-8→L+1 (26) |
| 24 | 333.9 | 0.0012 | H-9→L+1 (66), H-8→LUMO (20) |
| 25 | 332.8 | 0.0203 | H-13→L+1 (38), H-12→LUMO (49) |
| 26 | 331.8 | 0.0816 | H-13→LUMO (22), H-12→L+1 (36), H-11→L+1 (19), H-10→LUMO (18) |
| 27 | 331.6 | 0.0007 | H-11→LUMO (44), H-10→L+1 (45) |
| 28 | 331.6 | 0.0499 | H-13→LUMO (27), H-12→L+1 (10), H-11→L+1 (32), H-10→LUMO (26) |
| 29 | 316.1 | 0.0013 | H-15→L+1 (42), H-14→LUMO (51) |
| 30 | 315.4 | 0.1069 | H-15→LUMO (49), H-14→L+1 (44) |
| 31 | 311.9 | 0.0011 | H-13→L+1 (50), H-12→LUMO (45) |
| 32 | 311.9 | 0.0002 | H-13→LUMO (46), H-12→L+1 (50) |
| 33 | 304.1 | 0.0057 | H-16→LUMO (22), H-15→LUMO (36), H-14→L+1 (40) |
| 34 | 303.8 | 0.0014 | H-15→L+1 (52), H-14→LUMO (43) |
| 35 | 302.5 | 0.0247 | H-16→LUMO (70), H-15→LUMO (11), H-14→L+1 (13) |
| 36 | 301.0 | 0.0348 | H-16→L+1 (90) |
| 37 | 285.3 | 0.2431 | H-1→L+3 (50), HOMO→L+4 (41) |
| 38 | 285.1 | 0.2401 | H-7→L+2 (18), H-2→L+2 (59) |

| | | | |
|----|-------|--------|--|
| 39 | 282.9 | 0.4341 | H-1→L+4 (25), HOMO→L+3 (44), HOMO→L+5 (23) |
| 40 | 280.9 | 0.0028 | H-3→L+2 (36), H-1→L+5 (55) |
| 41 | 280.1 | 0.0135 | H-3→L+2 (62), H-1→L+5 (31) |
| 42 | 279.8 | 0.1399 | H-2→L+2 (21), H-1→L+4 (12), HOMO→L+5 (56) |
| 43 | 275.9 | 0.0001 | H-1→L+3 (44), HOMO→L+4 (50) |
| 44 | 275.9 | 0.0006 | H-1→L+4 (51), HOMO→L+3 (43) |
| 45 | 273.3 | 0.0036 | H-7→L+2 (57), H-2→L+2 (17) |
| 46 | 270.1 | 0.112 | H-17→L+1 (11), H-6→L+2 (15), H-4→L+2 (57) |
| 47 | 268.9 | 0 | H-5→L+2 (51), H-1→L+6 (29), HOMO→L+7 (11) |
| 48 | 268.4 | 0.0026 | H-5→L+2 (39), H-1→L+6 (36), HOMO→L+7 (15) |
| 49 | 268.2 | 0.0074 | H-4→L+2 (31), H-1→L+7 (14), HOMO→L+6 (40) |
| 50 | 267.6 | 0.1496 | H-17→L+1 (29), H-6→L+2 (27), H-4→L+2 (10), HOMO→L+6 (21) |
| 51 | 264.8 | 0.0799 | H-17→LUMO (94) |
| 52 | 262.8 | 0.0012 | H-1→L+6 (25), HOMO→L+7 (59) |
| 53 | 262.7 | 0.003 | H-1→L+7 (59), HOMO→L+6 (21) |
| 54 | 262.1 | 0.0909 | H-17→L+1 (48), H-6→L+2 (36) |
| 55 | 254.8 | 0.0027 | H-3→L+4 (12), H-2→L+3 (13), H-1→L+9 (16), HOMO→L+8 (20), HOMO→L+10 (15) |
| 56 | 254.8 | 0 | H-3→L+3 (14), H-2→L+4 (13), H-1→L+8 (15), H-1→L+10 (16), HOMO→L+9 (17) |
| 57 | 253.6 | 0.0094 | HOMO→L+8 (67) |
| 58 | 253.5 | 0.0004 | H-1→L+8 (56) |
| 59 | 253.5 | 0.001 | H-1→L+11 (24), HOMO→L+12 (23) |
| 60 | 253.4 | 0.0012 | H-1→L+8 (17), H-1→L+12 (21), HOMO→L+11 (21) |
| 61 | 247.0 | 0.017 | H-18→LUMO (13), H-8→L+2 (66) |
| 62 | 245.0 | 0.0006 | H-10→L+2 (94) |
| 63 | 244.6 | 0.011 | H-11→L+2 (91) |
| 64 | 243.8 | 0.0667 | H-18→LUMO (72), H-8→L+2 (12) |
| 65 | 242.8 | 0.1485 | H-18→L+1 (67), H-9→L+2 (17) |
| 66 | 241.6 | 0.0166 | H-18→L+1 (20), H-9→L+2 (69) |
| 67 | 240.7 | 0.0023 | H-3→L+3 (24), H-2→L+4 (26), H-1→L+10 (18), HOMO→L+9 (19) |
| 68 | 240.7 | 0.0739 | H-3→L+4 (21), H-2→L+3 (29), H-1→L+9 (19), HOMO→L+10 (18) |
| 69 | 237.2 | 0.0427 | H-19→LUMO (75) |
| 70 | 237.0 | 0.0922 | H-19→L+1 (63) |
| 71 | 236.8 | 0.0023 | H-1→L+11 (45), HOMO→L+12 (32) |
| 72 | 236.8 | 0.0013 | H-1→L+12 (38), HOMO→L+11 (39) |
| 73 | 236.7 | 0.0287 | H-19→L+1 (18), H-2→L+5 (26), HOMO→L+12 (15) |
| 74 | 236.2 | 0.0234 | H-5→L+4 (11), H-4→L+3 (11), H-3→L+5 (16), H-1→L+12 (16), HOMO→L+11 (10) |
| 75 | 235.3 | 0 | H-1→L+9 (32), H-1→L+10 (10), HOMO→L+10 (3) |

Table 7. Computed oscillator strengths (F), positions of the first electronic transitions and major contributions of **DPA-OMe (8)**.

| Transition No. | Wavelength (nm) | Osc. Strength | Major contributors (%) |
|----------------|-----------------|---------------|---|
| 1 | 574.3 | 0.0129 | H-1→L+1 (20), HOMO→LUMO (74) |
| 2 | 572.4 | 0.0078 | H-1→LUMO (31), HOMO→L+1 (63) |
| 3 | 537.7 | 0.018 | H-2→LUMO (18), H-1→L+1 (71), HOMO→LUMO (10) |
| 4 | 532.8 | 0.2454 | H-2→L+1 (47), H-1→LUMO (44) |
| 5 | 515.8 | 0.0274 | H-2→LUMO (76), HOMO→LUMO (14) |
| 6 | 503.5 | 0.8822 | H-2→L+1 (46), H-1→LUMO (23), HOMO→L+1 (28) |
| 7 | 442.9 | 0.0209 | HOMO→L+2 (98) |
| 8 | 439.2 | 0.0174 | H-1→L+2 (99) |
| 9 | 432.1 | 0.0517 | H-4→LUMO (54), H-3→L+1 (45) |
| 10 | 429.9 | 0.129 | H-4→L+1 (39), H-3→LUMO (59) |
| 11 | 411.7 | 0.0005 | H-4→LUMO (44), H-3→L+1 (54) |
| 12 | 411.6 | 0.0039 | H-4→L+1 (59), H-3→LUMO (39) |
| 13 | 405.5 | 0.0006 | H-6→LUMO (47), H-5→L+1 (50) |
| 14 | 403.8 | 0.1062 | H-6→L+1 (33), H-5→LUMO (62) |
| 15 | 388.0 | 0.0156 | H-6→LUMO (43), H-5→L+1 (38), H-2→L+2 (16) |
| 16 | 387.5 | 0.0022 | H-6→L+1 (64), H-5→LUMO (34) |
| 17 | 387.3 | 0.1153 | H-2→L+2 (80) |
| 18 | 355.1 | 0.0007 | H-11→L+1 (12), H-10→LUMO (44), H-9→L+1 (41) |
| 19 | 355.0 | 0.0673 | H-11→LUMO (11), H-10→L+1 (33), H-9→LUMO (53) |
| 20 | 349.0 | 0.0234 | H-8→L+1 (21), H-7→LUMO (69) |
| 21 | 344.2 | 0.195 | H-8→LUMO (31), H-7→L+1 (58) |
| 22 | 342.8 | 0.0141 | H-11→LUMO (39), H-10→L+1 (14), H-9→LUMO (34) |
| 23 | 341.3 | 0.0241 | H-11→L+1 (29), H-10→LUMO (14), H-9→L+1 (47) |
| 24 | 336.8 | 0 | H-8→LUMO (54), H-7→L+1 (36) |
| 25 | 336.3 | 0 | H-8→L+1 (66), H-7→LUMO (26) |
| 26 | 334.5 | 0.0018 | H-3→L+2 (99) |
| 27 | 334.4 | 0 | H-4→L+2 (98) |
| 28 | 331.2 | 0 | H-11→LUMO (41), H-10→L+1 (43) |
| 29 | 330.8 | 0.0006 | H-11→L+1 (54), H-10→LUMO (34) |
| 30 | 330.2 | 0.007 | H-14→LUMO (18), H-13→L+1 (42), H-12→LUMO (31) |
| 31 | 329.1 | 0.1027 | H-14→L+1 (12), H-13→LUMO (48), H-12→L+1 (29) |
| 32 | 321.0 | 0.0009 | H-5→L+2 (67) |
| 33 | 318.6 | 0.0078 | H-9→L+2 (18), H-5→L+2 (29), H-2→L+3 (14), HOMO→L+3 (14) |
| 34 | 318.2 | 0 | H-6→L+2 (95) |
| 35 | 316.4 | 0.0084 | H-15→LUMO (37), H-14→L+1 (32), H-12→L+1 (19) |
| 36 | 316.0 | 0.0717 | H-15→L+1 (13), H-14→LUMO (33), H-12→LUMO (28) |
| 37 | 313.0 | 0.0002 | H-13→LUMO (42), H-12→L+1 (42) |
| 38 | 313.0 | 0.0242 | H-16→LUMO (10), H-14→LUMO (14), H-13→L+1 (50), H-12→LUMO (19) |
| 39 | 312.5 | 0.0318 | H-16→LUMO (53), H-15→L+1 (26) |

| | | | |
|----|-------|--------|---|
| 40 | 311.4 | 0.0213 | H-16→L+1 (55), H-15→LUMO (21), H-14→L+1 (20) |
| 41 | 305.9 | 0.0028 | H-16→LUMO (22), H-15→L+1 (47), H-14→LUMO (22) |
| 42 | 305.6 | 0.0055 | H-16→L+1 (36), H-15→LUMO (31), H-14→L+1 (24) |
| 43 | 298.0 | 0.0944 | H-1→L+3 (99) |
| 44 | 297.4 | 0.0719 | H-2→L+3 (16), HOMO→L+3 (71) |
| 45 | 288.0 | 0.0087 | H-7→L+2 (72) |
| 46 | 285.4 | 0.0129 | H-11→L+2 (49), H-9→L+2 (35) |
| 47 | 285.3 | 0.0037 | H-10→L+2 (88) |
| 48 | 282.7 | 0.0738 | H-1→L+4 (48), HOMO→L+5 (31) |
| 49 | 282.7 | 0.0669 | H-8→L+2 (77), HOMO→L+4 (10) |
| 50 | 281.0 | 0.4438 | H-8→L+2 (14), HOMO→L+4 (74) |
| 51 | 277.9 | 0.0037 | H-1→L+4 (18), HOMO→L+5 (37), HOMO→L+6 (29) |
| 52 | 276.4 | 0.0922 | H-1→L+5 (81), HOMO→L+4 (11) |
| 53 | 276.2 | 0.0035 | H-1→L+4 (24), HOMO→L+5 (21), HOMO→L+6 (31) |
| 54 | 272.6 | 0.0189 | H-1→L+6 (79) |
| 55 | 271.8 | 0.0115 | H-15→L+2 (11), H-13→L+2 (87) |
| 56 | 271.6 | 0.0052 | H-14→L+2 (32), H-12→L+2 (66) |
| 57 | 270.2 | 0.0005 | H-16→L+2 (25), H-2→L+6 (11), HOMO→L+6 (25) |
| 58 | 268.5 | 0.0032 | H-1→L+8 (38), HOMO→L+7 (54) |
| 59 | 267.6 | 0.0059 | H-16→L+2 (10), H-1→L+7 (19), HOMO→L+8 (52) |
| 60 | 264.1 | 0.0007 | H-1→L+8 (53), HOMO→L+7 (33) |
| 61 | 264.1 | 0.0001 | H-1→L+7 (65), HOMO→L+8 (19) |
| 62 | 262.8 | 0.0403 | H-16→L+2 (17), H-14→L+2 (37), H-12→L+2 (19), H-11→L+2 (11) H-15→L+2 (85) |
| 63 | 262.3 | 0 | H-17→L+1 (28), H-2→L+5 (11), H-2→L+6 (17) |
| 64 | 260.2 | 0.335 | H-2→L+4 (93) |
| 65 | 260.1 | 0.024 | H-2→L+3 (12), H-2→L+5 (68) |
| 66 | 259.2 | 0.0859 | H-17→LUMO (83) |
| 67 | 256.2 | 0.08 | H-17→L+1 (38), H-16→L+2 (10), H-2→L+6 (23) |
| 68 | 255.9 | 0.0224 | H-4→L+5 (11), H-3→L+4 (16), H-1→L+9 (19), HOMO→L+11 (17) |
| 69 | 254.1 | 0.0006 | H-4→L+4 (14), H-3→L+5 (11), H-1→L+11 (14), HOMO→L+9 (19) |
| 70 | 254.0 | 0.0064 | H-18→LUMO (10), H-1→L+10 (20), HOMO→L+12 (19) |
| 71 | 253.0 | 0.0065 | H-18→L+1 (10), H-1→L+12 (17), HOMO→L+10 (22) |
| 72 | 252.9 | 0.003 | H-18→LUMO (34), H-2→L+6 (21) |
| 73 | 249.7 | 0.4864 | H-2→L+6 (15), H-2→L+8 (72) |
| 74 | 247.8 | 0.0734 | H-2→L+7 (93) |
| 75 | 247.5 | 0.0128 | |

Table 8. Computed oscillator strengths (F), positions of the first electronic transitions and major contributions of **DPO-O (9)**.

| Transition No. | Wavelength (nm) | Osc. Strength | Major contributors (%) |
|----------------|-----------------|---------------|---|
| 1 | 597.5 | 0.0001 | H-1→L+1 (38), HOMO→LUMO (62) |
| 2 | 597.2 | 0.0018 | H-1→LUMO (55), HOMO→L+1 (45) |
| 3 | 571.3 | 0.0066 | H-1→L+1 (62), HOMO→LUMO (37) |
| 4 | 559.1 | 0.7257 | H-1→LUMO (45), HOMO→L+1 (54) |
| 5 | 472.6 | 0.0656 | H-3→LUMO (44), H-2→L+1 (55) |
| 6 | 467.3 | 0.2492 | H-3→L+1 (36), H-2→LUMO (62) |
| 7 | 444.7 | 0.0032 | H-3→LUMO (55), H-2→L+1 (43) |
| 8 | 444.4 | 0 | H-3→L+1 (61), H-2→LUMO (37) |
| 9 | 404.9 | 0.0337 | H-6→L+1 (10), H-5→L+1 (49), H-4→LUMO (37) |
| 10 | 403.9 | 0.0379 | H-5→LUMO (53), H-4→L+1 (43) |
| 11 | 401.6 | 0.1527 | H-6→L+1 (69), H-4→LUMO (19) |
| 12 | 398.7 | 0.1502 | H-6→LUMO (82), H-5→LUMO (10) |
| 13 | 396.0 | 0.0055 | H-7→LUMO (78) |
| 14 | 395.3 | 0.0834 | H-7→L+1 (85) |
| 15 | 380.9 | 0.0007 | H-7→LUMO (10), H-6→L+1 (14), H-5→L+1 (40), H-4→LUMO (36) |
| 16 | 380.9 | 0 | H-7→L+1 (12), H-6→LUMO (12), H-5→LUMO (33), H-4→L+1 (43) |
| 17 | 358.8 | 0.0269 | H-8→LUMO (87) |
| 18 | 356.4 | 0.0109 | H-8→L+1 (25), HOMO→L+2 (70) |
| 19 | 355.6 | 0.016 | H-1→L+2 (97) |
| 20 | 355.5 | 0.0626 | H-8→L+1 (58), HOMO→L+2 (28) |
| 21 | 346.9 | 0.0017 | H-11→LUMO (50), H-10→L+1 (46) |
| 22 | 346.7 | 0.0268 | H-11→L+1 (45), H-10→LUMO (52) |
| 23 | 339.9 | 0.0197 | H-13→L+1 (26), H-12→LUMO (26), H-9→L+1 (38) |
| 24 | 339.7 | 0.0277 | H-13→LUMO (15), H-12→L+1 (11), H-9→LUMO (58), H-8→L+1 (11) |
| 25 | 335.0 | 0.0735 | H-13→LUMO (31), H-12→L+1 (29), H-9→LUMO (27) |
| 26 | 334.9 | 0.008 | H-13→L+1 (17), H-12→LUMO (23), H-9→L+1 (49) |
| 27 | 323.7 | 0.0002 | H-11→LUMO (41), H-10→L+1 (46) |
| 28 | 323.7 | 0.0001 | H-11→L+1 (45), H-10→LUMO (41) |
| 29 | 313.2 | 0 | H-13→L+1 (44), H-12→LUMO (42) |
| 30 | 313.1 | 0.0001 | H-13→LUMO (40), H-12→L+1 (47) |
| 31 | 306.1 | 0.2006 | H-14→LUMO (20), H-1→L+4 (30), HOMO→L+3 (37) |
| 32 | 301.4 | 0.5938 | H-16→L+1 (13), H-15→LUMO (19), H-14→L+1 (14), H-1→L+3 (19), HOMO→L+4 (16) |
| 33 | 300.9 | 0.0083 | H-16→LUMO (42), H-15→L+1 (34) |
| 34 | 300.8 | 0.4839 | H-16→L+1 (22), H-15→LUMO (23), H-14→L+1 (12), H-1→L+3 (13), HOMO→L+4 (12) |
| 35 | 297.6 | 0.0011 | H-1→L+4 (35), HOMO→L+3 (56) |
| 36 | 297.5 | 0.0019 | H-1→L+3 (46), HOMO→L+4 (53) |
| 37 | 296.7 | 0.1778 | H-14→L+1 (46), H-2→L+2 (35) |

| | | | |
|----|-------|--------|---|
| 38 | 296.5 | 0.0153 | H-14→LUMO (63), H-1→L+4 (28) |
| 39 | 291.3 | 0.0786 | H-14→L+1 (23), H-2→L+2 (54) |
| 40 | 289.6 | 0.009 | H-3→L+2 (94) |
| 41 | 287.8 | 0.0001 | H-16→L+1 (53), H-15→LUMO (45) |
| 42 | 287.8 | 0.0001 | H-16→LUMO (45), H-15→L+1 (52) |
| 43 | 285.8 | 0.0202 | HOMO→L+5 (79) |
| 44 | 285.4 | 0.0012 | H-1→L+5 (76) |
| 45 | 276.4 | 0.0005 | HOMO→L+6 (76) |
| 46 | 276.1 | 0.0183 | H-1→L+6 (75) |
| 47 | 273.3 | 0.005 | H-6→L+2 (50), H-5→L+2 (17) |
| 48 | 272.4 | 0.1015 | H-3→L+4 (34), H-2→L+3 (39) |
| 49 | 272.3 | 0.0107 | H-3→L+3 (30), H-2→L+4 (31) |
| 50 | 271.5 | 0.0011 | H-1→L+6 (10), HOMO→L+7 (71) |
| 51 | 271.2 | 0.0001 | H-1→L+7 (68) |
| 52 | 267.1 | 0.2147 | H-17→L+1 (49), H-7→L+2 (30), H-4→L+2 (10) |
| 53 | 264.0 | 0.0354 | H-17→LUMO (90) |
| 54 | 262.5 | 0.0129 | H-17→L+1 (10), H-4→L+2 (75) |
| 55 | 262.2 | 0.0072 | H-6→L+2 (24), H-5→L+2 (71) |
| 56 | 260.7 | 0.037 | H-7→L+2 (15), H-4→L+2 (10), H-1→L+10 (17), HOMO→L+9 (13) |
| 57 | 260.2 | 0.0317 | H-2→L+6 (10), H-1→L+9 (18), HOMO→L+10 (23) |
| 58 | 259.8 | 0.0742 | H-17→L+1 (32), H-7→L+2 (33) |
| 59 | 258.4 | 0 | HOMO→L+8 (88) |
| 60 | 258.2 | 0.0074 | H-1→L+8 (88) |
| 61 | 254.8 | 0.0027 | H-3→L+4 (47), H-2→L+3 (49) |
| 62 | 254.8 | 0.0002 | H-3→L+3 (47), H-2→L+4 (50) |
| 63 | 254.3 | 0 | H-19→L+1 (46), H-18→LUMO (49) |
| 64 | 254.3 | 0.004 | H-19→LUMO (49), H-18→L+1 (45) |
| 65 | 251.3 | 0.0015 | H-8→L+2 (76), H-7→L+2 (10) |
| 66 | 248.4 | 0.0023 | H-22→LUMO (20), H-21→L+1 (24), H-2→L+5 (18) |
| 67 | 248.4 | 0 | H-22→L+1 (20), H-21→LUMO (27), H-3→L+5 (14), H- 2→L+6 (10) |
| 68 | 247.8 | 0.0154 | H-1→L+11 (31), HOMO→L+12 (35) |
| 69 | 247.7 | 0.3337 | H-1→L+12 (32), HOMO→L+11 (33) |
| 70 | 245.7 | 0.0069 | H-22→LUMO (13), H-21→L+1 (16), H-2→L+5 (34) |
| 71 | 245.4 | 0.0334 | H-22→L+1 (13), H-21→LUMO (16), H-3→L+5 (28), H- 2→L+6 (16) |
| 72 | 242.9 | 0.0504 | H-9→L+2 (54) |
| 73 | 241.8 | 0.0145 | H-5→L+3 (27), H-4→L+4 (28), H-1→L+10 (10), HOMO→L+9 (14) |
| 74 | 241.8 | 0 | H-5→L+4 (22), H-4→L+3 (26), H-1→L+9 (10), HOMO→L+10 (20) |
| 75 | 241.4 | 0.1024 | H-3→L+6 (30), H-2→L+5 (22), H-2→L+7 (18) |

Table 9. Computed oscillator strengths (F), positions of the first electronic transitions and major contributions of **DPA-O (10)**.

| Transition No. | Wavelength (nm) | Osc. Strength | Major contributors (%) |
|----------------|-----------------|---------------|---|
| 1 | 608.8 | 0.0137 | H-1→L+1 (20), HOMO→LUMO (79) |
| 2 | 605.8 | 0.0038 | H-1→LUMO (48), HOMO→L+1 (51) |
| 3 | 572.3 | 0.0057 | H-1→L+1 (79), HOMO→LUMO (19) |
| 4 | 561.6 | 0.478 | H-2→L+1 (16), H-1→LUMO (46), HOMO→L+1 (37) |
| 5 | 532.9 | 0.1779 | H-2→LUMO (97) |
| 6 | 530.6 | 0.2299 | H-2→L+1 (82), HOMO→L+1 (12) |
| 7 | 463.2 | 0.0117 | H-4→L+1 (23), H-3→LUMO (76) |
| 8 | 458.7 | 0.1315 | H-4→LUMO (49), H-3→L+1 (47) |
| 9 | 450.4 | 0.0064 | HOMO→L+2 (97) |
| 10 | 447.2 | 0.0328 | H-1→L+2 (99) |
| 11 | 440.1 | 0.0129 | H-4→LUMO (49), H-3→L+1 (50) |
| 12 | 438.5 | 0.0004 | H-4→L+1 (76), H-3→LUMO (23) |
| 13 | 400.6 | 0.0031 | H-6→LUMO (60), H-5→L+1 (37) |
| 14 | 399.7 | 0.1188 | H-6→L+1 (35), H-5→LUMO (62) |
| 15 | 389.8 | 0.1068 | H-2→L+2 (95) |
| 16 | 382.7 | 0.0006 | H-6→LUMO (38), H-5→L+1 (61) |
| 17 | 382.6 | 0.0027 | H-6→L+1 (63), H-5→LUMO (36) |
| 18 | 366.3 | 0.0418 | H-7→LUMO (88) |
| 19 | 358.9 | 0.1823 | H-7→L+1 (82) |
| 20 | 348.6 | 0.0055 | H-9→LUMO (21), H-3→L+2 (68) |
| 21 | 348.2 | 0.0059 | H-9→LUMO (59), H-3→L+2 (26) |
| 22 | 348.0 | 0.0007 | H-8→LUMO (79), H-7→L+1 (13) |
| 23 | 345.2 | 0.0003 | H-8→L+1 (77) |
| 24 | 345.1 | 0 | H-11→LUMO (38), H-10→L+1 (25), H-9→L+1 (31) |
| 25 | 342.7 | 0.0011 | H-4→L+2 (91) |
| 26 | 342.5 | 0.0218 | H-11→L+1 (32), H-10→LUMO (52), H-9→LUMO (10) |
| 27 | 339.4 | 0.0159 | H-11→LUMO (14), H-10→L+1 (14), H-9→L+1 (67) |
| 28 | 334.4 | 0.0141 | H-13→LUMO (50), H-12→L+1 (35) |
| 29 | 333.5 | 0.0744 | H-13→L+1 (32), H-12→LUMO (50) |
| 30 | 322.6 | 0.0001 | H-11→LUMO (38), H-10→L+1 (51) |
| 31 | 322.6 | 0.0002 | H-11→L+1 (53), H-10→LUMO (36) |
| 32 | 318.3 | 0.0596 | H-9→L+2 (21), HOMO→L+3 (46) |
| 33 | 314.7 | 0.0032 | H-13→LUMO (37), H-12→L+1 (45) |
| 34 | 314.3 | 0.001 | H-13→L+1 (53), H-12→LUMO (36) |
| 35 | 311.6 | 0.0518 | H-14→LUMO (31), H-9→L+2 (13), H-1→L+4 (11), HOMO→L+3 (13) |
| 36 | 308.8 | 0.0132 | H-6→L+2 (95) |
| 37 | 308.8 | 0.0031 | H-5→L+2 (89) |
| 38 | 308.2 | 0.2683 | H-1→L+3 (82) |
| 39 | 305.5 | 0.3524 | H-14→L+1 (61), HOMO→L+4 (26) |
| 40 | 305.0 | 0.0037 | H-14→LUMO (25), H-2→L+3 (11), HOMO→L+3 (35) |

| | | | |
|----|-------|--------|--|
| 41 | 301.1 | 0.0281 | H-14→LUMO (22), H-1→L+4 (63) |
| 42 | 300.5 | 0.0703 | H-1→L+5 (36), HOMO→L+4 (54) |
| 43 | 299.8 | 0.0145 | H-16→L+1 (14), H-15→LUMO (25), HOMO→L+5 (33) |
| 44 | 299.4 | 0.0001 | H-16→LUMO (45), H-15→L+1 (31), HOMO→L+7 (10) |
| 45 | 298.5 | 0.0029 | H-16→L+1 (13), H-15→LUMO (21), HOMO→L+5 (42) |
| 46 | 294.7 | 0.5997 | H-14→L+1 (23), H-1→L+5 (47), HOMO→L+4 (12) |
| 47 | 294.5 | 0.0045 | H-7→L+2 (79) |
| 48 | 288.5 | 0.0002 | H-16→LUMO (44), H-15→L+1 (54) |
| 49 | 288.4 | 0.0003 | H-16→L+1 (55), H-15→LUMO (43) |
| 50 | 283.7 | 0.0093 | H-8→L+2 (97) |
| 51 | 281.9 | 0.0071 | H-2→L+3 (15), H-2→L+5 (11), HOMO→L+6 (57) |
| 52 | 280.9 | 0.0121 | H-2→L+4 (49), H-1→L+6 (27), HOMO→L+7 (12) |
| 53 | 279.9 | 0.0247 | H-2→L+3 (27), H-2→L+5 (31), HOMO→L+6 (18) |
| 54 | 279.0 | 0.0118 | H-2→L+4 (32), H-1→L+6 (52) |
| 55 | 277.3 | 0.0001 | HOMO→L+7 (71) |
| 56 | 275.6 | 0.0364 | H-1→L+7 (79) |
| 57 | 273.4 | 0.0027 | H-10→L+2 (82) |
| 58 | 273.3 | 0.0302 | HOMO→L+8 (68) |
| 59 | 272.8 | 0.0081 | H-11→L+2 (89) |
| 60 | 271.7 | 0.0002 | H-1→L+8 (82) |
| 61 | 270.4 | 0 | H-4→L+4 (23), H-3→L+3 (35), H-3→L+5 (11) |
| 62 | 270.0 | 0.0759 | H-4→L+3 (22), H-3→L+4 (38) |
| 63 | 268.3 | 0.0373 | H-13→L+2 (77) |
| 64 | 267.9 | 0.035 | H-12→L+2 (93) |
| 65 | 265.8 | 0.0119 | H-14→L+2 (20), H-13→L+2 (16), H-2→L+6 (35), H-2→L+8 (15) |
| 66 | 261.8 | 0.0002 | H-2→L+7 (25), H-1→L+11 (14) |
| 67 | 261.4 | 0.028 | H-1→L+10 (10), HOMO→L+11 (15) |
| 68 | 258.8 | 0.2605 | H-17→L+1 (15), H-4→L+3 (32), H-3→L+4 (15) |
| 69 | 258.0 | 0.0016 | H-4→L+4 (30), H-3→L+3 (52) |
| 70 | 256.3 | 0.2567 | H-17→L+1 (25), H-4→L+3 (25), H-3→L+4 (22) |
| 71 | 256.2 | 0.0656 | H-2→L+7 (59) |
| 72 | 255.9 | 0.0147 | H-14→L+2 (28), H-2→L+6 (41) |
| 73 | 254.2 | 0.062 | H-17→LUMO (88) |
| 74 | 253.8 | 0.0078 | H-14→L+2 (25), H-2→L+8 (52) |
| 75 | 253.7 | 0.0024 | H-4→L+4 (21), H-3→L+5 (73) |

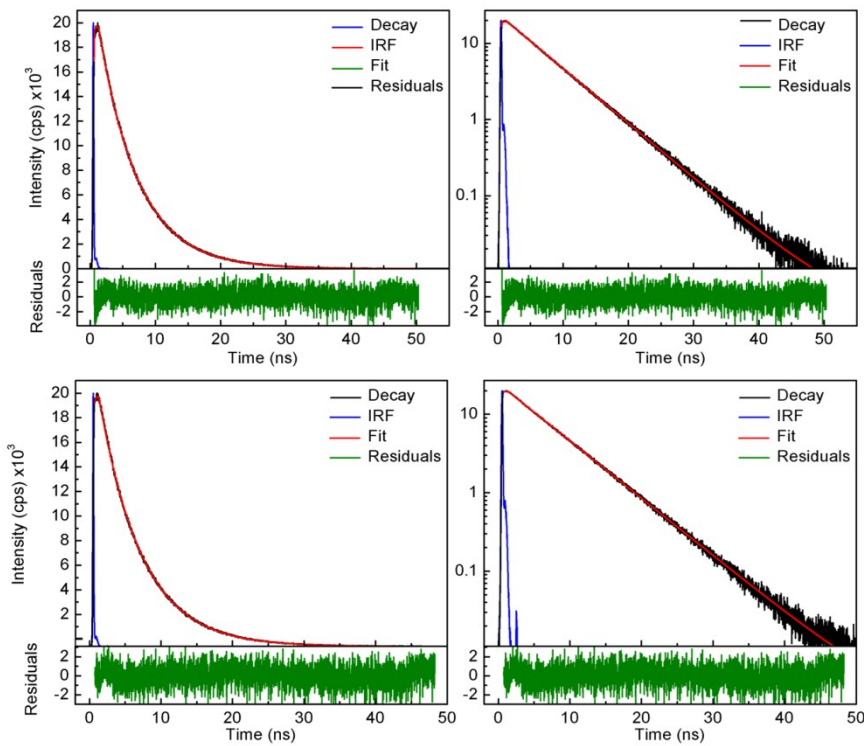


Figure S34. Fluorescence decay trace for **BOD-OMe (3)** at 298 (top) and 77 K (bottom). Decay traces are shown in both a liner and logarithmic scale.

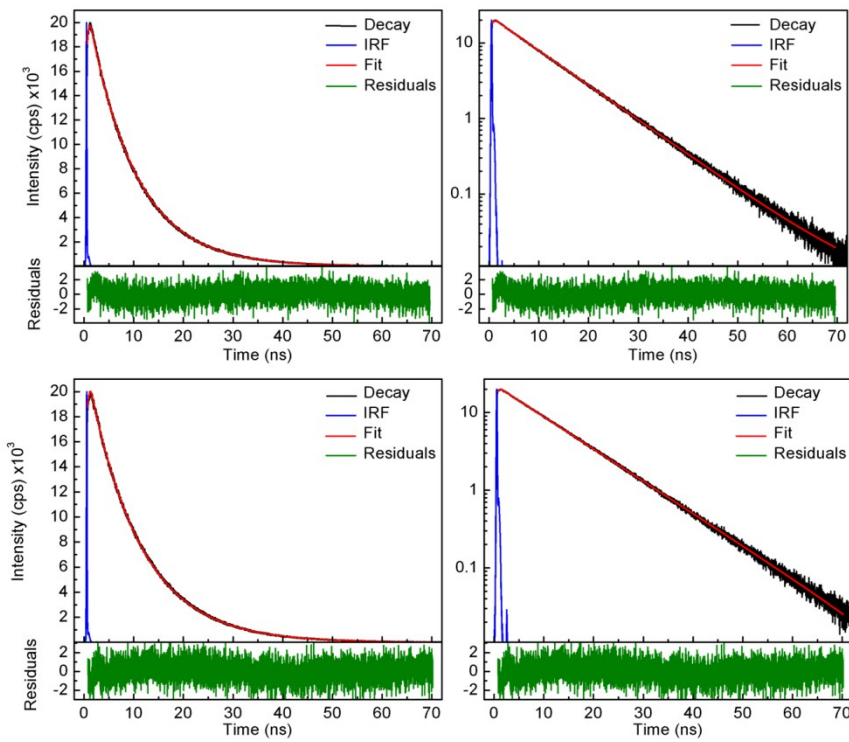


Figure S35. Fluorescence decay trace for **BOD-O (4)** at 298 (top) and 77 K (bottom). Decay traces are shown in both a liner and logarithmic scale.

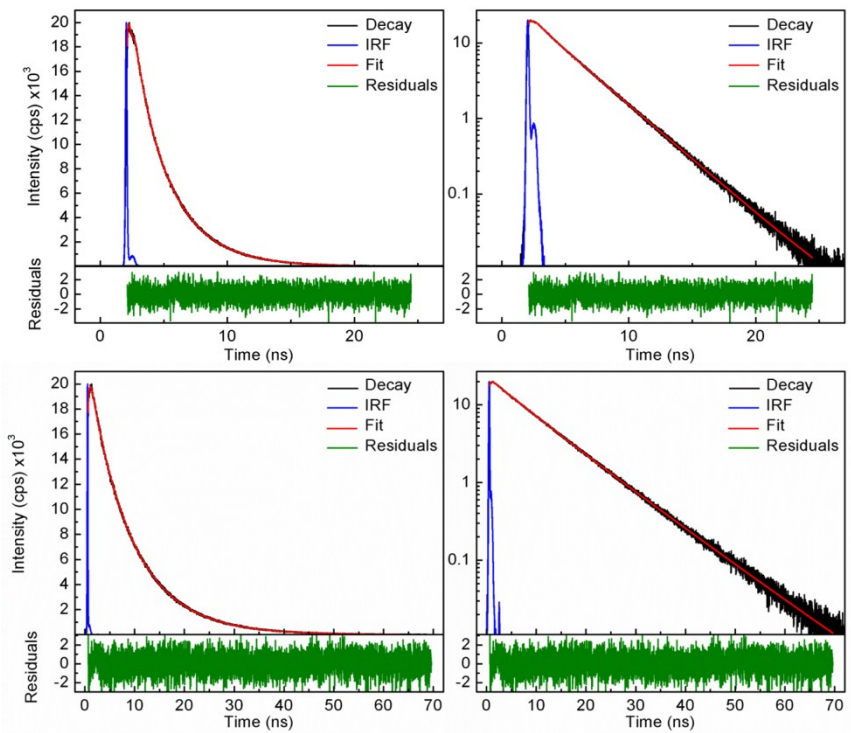


Figure S36. Fluorescence decay trace for **DPO-OMe (7)** at 298 (top) and 77 K (bottom). Decay traces are shown in both a liner and logarithmic scale.

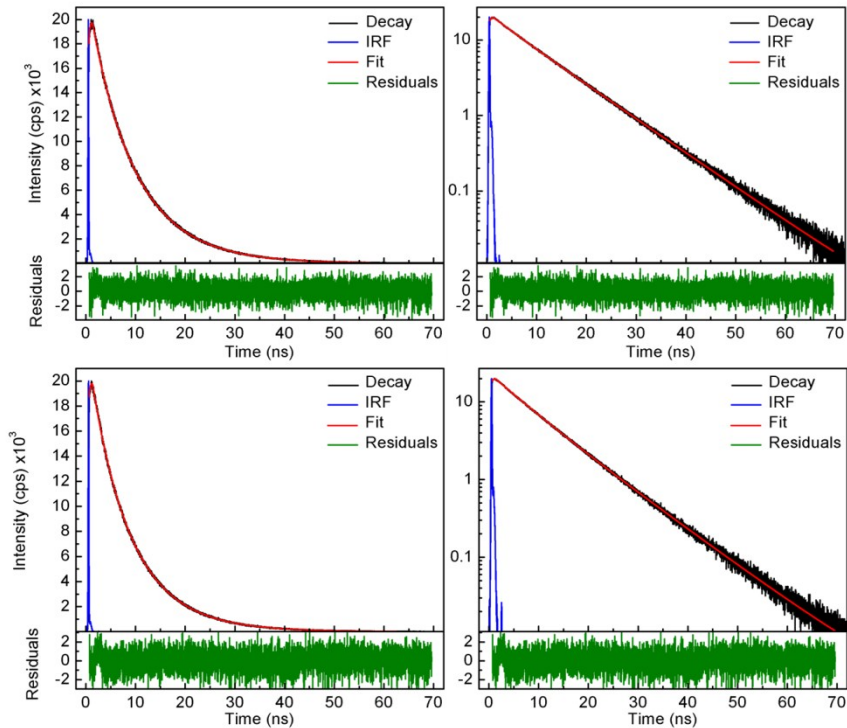


Figure S37. Fluorescence decay trace for **DPA-OMe (8)** at 298 (top) and 77 K (bottom). Decay traces are shown in both a liner and logarithmic scale.

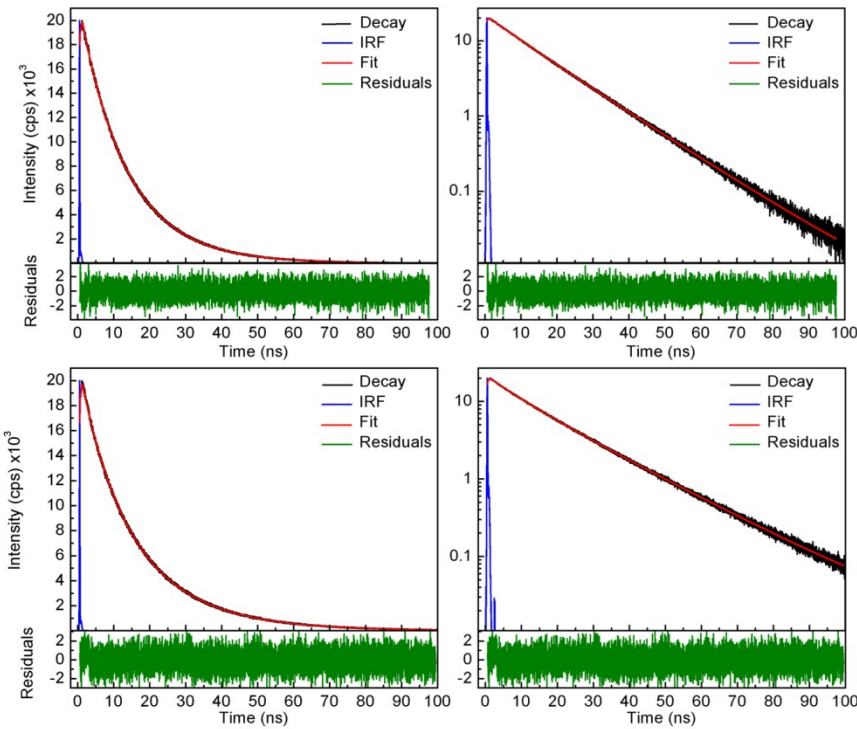


Figure S38. Fluorescence decay trace for **DPO-O (9)** at 298 (top) and 77 K (bottom). Decay traces are shown in both a liner and logarithmic scale.

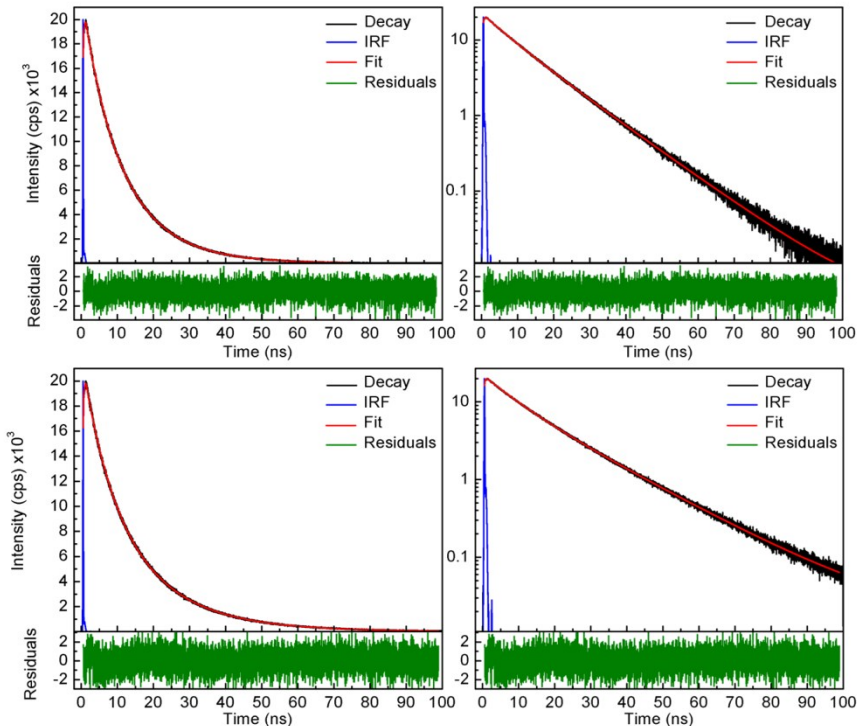


Figure S39. Fluorescence decay trace for **DPA-O (10)** at 298 (top) and 77 K (bottom). Decay traces are shown in both a liner and logarithmic scale.

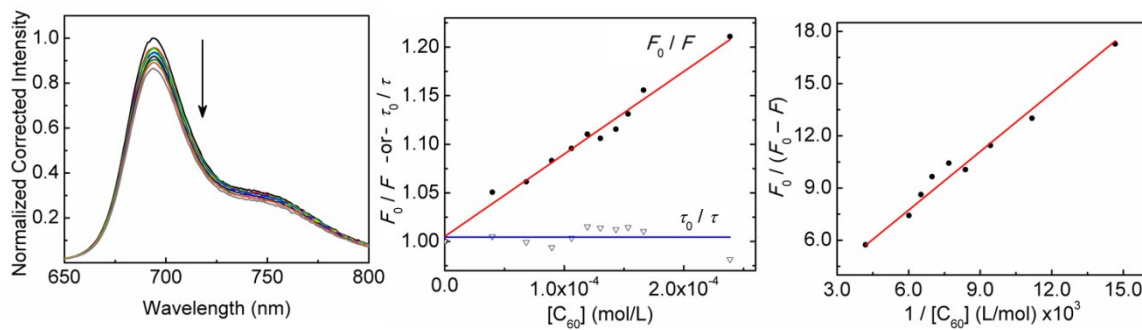


Figure S40. Left: evolution of fluorescence spectra of **BOD-O (4)** in 1,2-dichlorobenzene upon addition of C_60 . Middle: Stern-Volmer analysis of fluorescence quenching of **BOD-O (4)** by C_60 in 1,2-dichlorobenzene. Right: Modified Stern-Volmer analysis. See SI for the five other compounds. The C_60 concentration was increased from 0 to 5.5 equivalents.

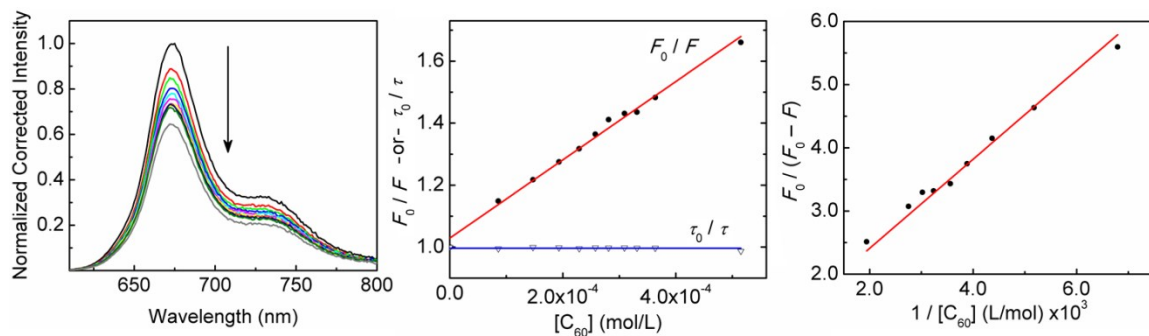


Figure S41. Left: evolution of fluorescence spectra of **DPO-OMe (7)** in 1,2-dichlorobenzene upon addition of C_60 . Middle: Stern-Volmer analysis of fluorescence quenching of **DPO-OMe (7)** by C_60 in 1,2-dichlorobenzene. Right: Modified Stern-Volmer analysis. See SI for the five other compounds. The C_60 concentration was increased from 0 to 26.4 equivalents.

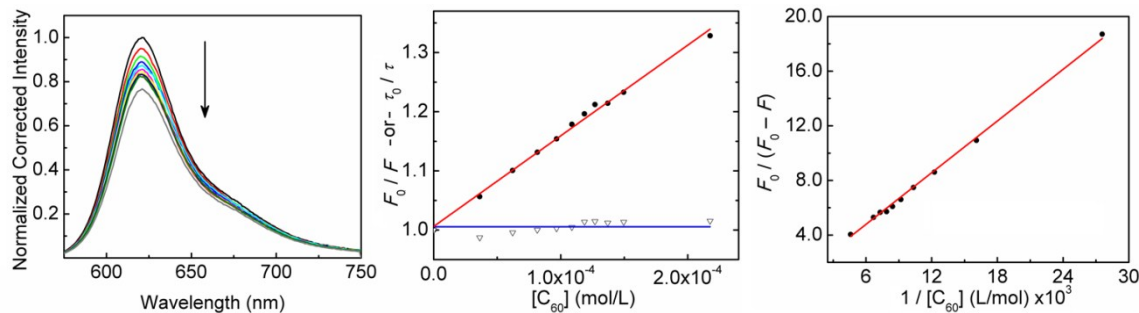


Figure S42. Left: evolution of fluorescence spectra of **DPA-OMe (8)** in 1,2-dichlorobenzene upon addition of C_60 . Middle: Stern-Volmer analysis of fluorescence quenching of **DPA-OMe (8)** by C_60 in 1,2-dichlorobenzene. Right: Modified Stern-Volmer analysis. See SI for the five other compounds. The C_60 concentration was increased from 0 to 15.0 equivalents.

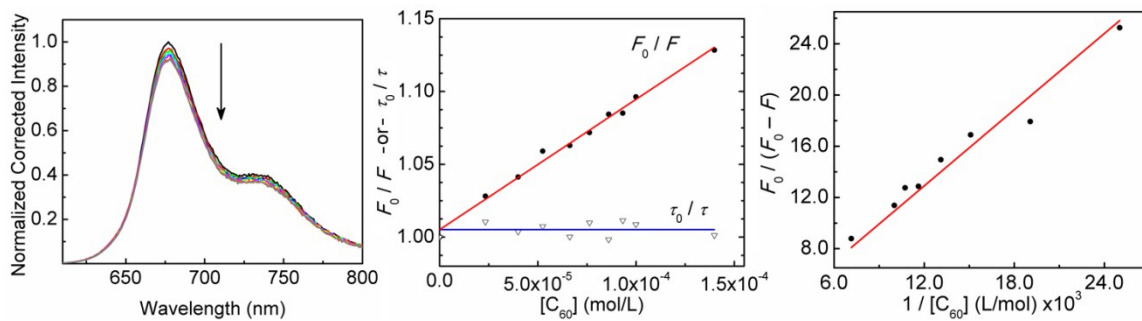


Figure S43. Left: evolution of fluorescence spectra of **DPO-O (9)** in 1,2-dichlorobenzene upon addition of C₆₀. Middle: Stern-Volmer analysis of fluorescence quenching of **DPO-O (9)** by C₆₀ in 1,2-dichlorobenzene. Right: Modified Stern-Volmer analysis. See SI for the five other compounds. The C₆₀ concentration was increased from 0 to 10.0 equivalents.

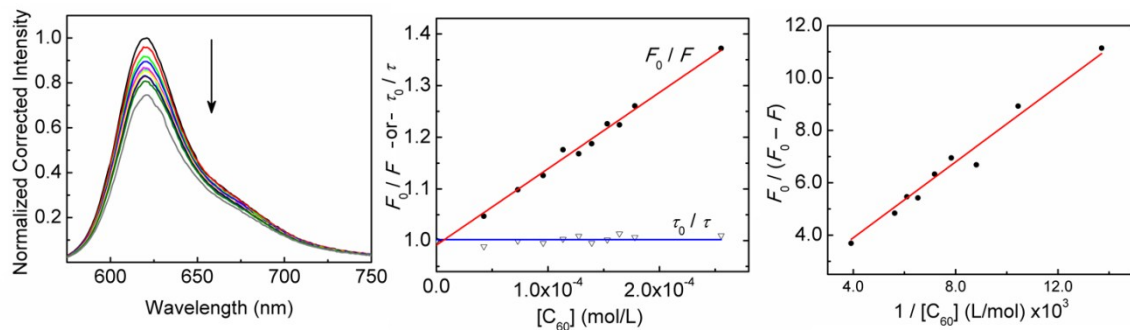


Figure S44. Left: evolution of fluorescence spectra of **DPA-O (10)** in 1,2-dichlorobenzene upon addition of C₆₀. Middle: Stern-Volmer analysis of fluorescence quenching of **DPA-O (10)** by C₆₀ in 1,2-dichlorobenzene. Right: Modified Stern-Volmer analysis. See SI for the five other compounds. The C₆₀ concentration was increased from 0 to 15.3 equivalents.